Royal Netherlands
Meteorological Institute
Ministry of Infrastructure and the Environment

North Sea wind climatology
Part 1: a review of existing wind atlases

I.L. Wijnant, H.W. van den Brink and A. Stepek

De Bilt, 2014 | Technical report; TR-342

North Sea wind climatology
Part 1: a review of existing wind atlases

I.L. Wijnant, H.W. van den Brink and A. Stepek
June 2014

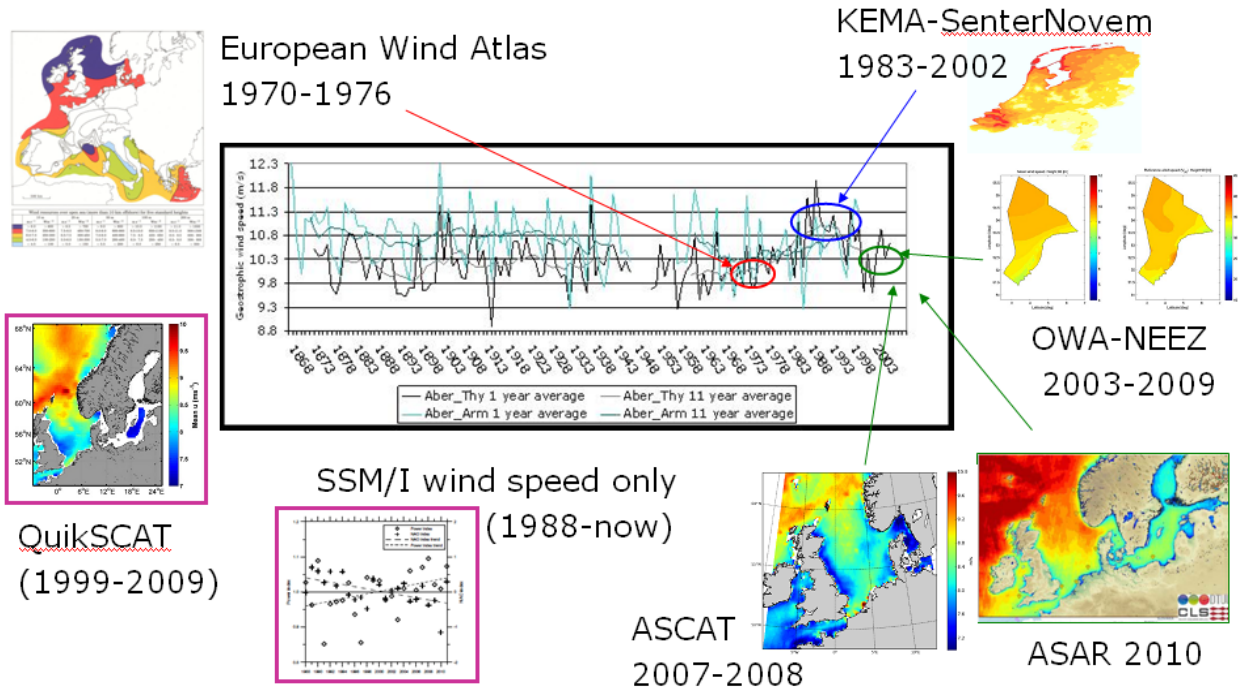

North Sea wind climatology: a review of existing wind atlases

Executive Summary

The national government needs high quality offshore wind climatology at and around hub height to be able to determine a realistic wind power potential for the North Sea and to be able to assess whether the yields predicted by wind energy companies are reliable. One "reference" wind atlas makes procedures more transparent for all stages in the process of establishing Dutch offshore wind energy: allocation of areas, tendering procedure, allocation of wind energy producer and monitoring of the wind energy yields. It will also save time and money as individual wind energy companies would not have to make their own wind climatologies. It is however essential that the quality of this "reference" wind atlas is scientifically sound and that it has the confidence of the wind energy sector and the banks (so they would be willing to lend the required funds).

Wind energy developers determine wind climatology at the site where they want to build the wind turbine or wind farm (target site) by transforming long series of near surface wind measurements at a nearby reference site, if available, to hub height at the target site. The transformation requires simultaneous measurements at both sites, but the measurement campaigns at the target site are relatively short. This is called the Measure Correlate Predict (MCP) method. The main problem with using measurements as reference data is that they are predominantly done at levels below hub height. To bridge the height difference between the reference and target measurements, assumptions have to made on the atmospheric stability and the associated vertical wind profile. The temperature profiles required for deriving the actual atmospheric stability are only measured at a few wind masts and for a limited period.

Wind atlases are used for siting purposes. This report gives an overview of the main wind atlases used in the wind energy sector and explains their limitations:

- The existing wind atlases do not include the long-term variability of the wind climate because they are based on short measurement campaigns or short periods of weather forecasting model output. The European Wind Atlas, the OWA-NEEZ wind atlas and the NORSEWInD (based on SAR and ASCAT satellite wind measurements) wind atlases are based on relatively calm periods, the KEMA/SenterNovem Wind Atlas on a relatively windy period. The only wind atlas based on a period in which most of the long-term wind speed variability is captured is the NORSEWInD QuikSCAT map that is based on satellite observations from 1999-2009, but sampling[1] and quality control[2] errors in the map are not yet accounted for. This is because the NORSEWInD project lacked the financial resources to perform a collocation procedure.
- Most existing wind atlases do not provide information above 100 m (only the European Wind Atlas gives information up to a level of 200m, but the information above 200 m is of limited value).
- As most existing wind atlases are based on measurements at 10 m above the ground or at the sea surface (satellite measurements), these observations have to be extrapolated to higher levels and assumptions have to be made on the influence of atmospheric stability on the wind profile.
  - WAsP based atlases (European Wind Atlases and KEMA/SenterNovem Wind Atlas): both the extrapolation formula (Businger-Dyer) and the empirical function (stability function Ψm) that is used to describe the effect of stability on the wind profile have been improved since they were used in the WAsP-based wind atlases. The effect of the height of the planetary boundary layer should e.g. be included in the extrapolation formula (adapted Businger-Dyer). Furthermore, only a climatological average of the non-neutral stability effects is used, which means that hour to hour stability effects on the wind profile can not be reproduced and time series of the wind speed at

[1] Satellite observations are only made a few times a day and do not represent the average of the full diurnal cycle.
[2] The back scattered radar signal is e.g. disturbed by large numbers of ships waiting at the anchor places near main harbours. Quality Control screens some of the ship-reflection contaminated observations at low winds, but less so at high wind speeds (reduced contrast).

hub height can not be estimated accurately. Finally, there is only one climatological average wind profile for land and one for sea, whereas in reality it varies from location to location. In contrast, wind data from weather forecasting models do not suffer from either limitation.
  - Satellite based wind atlases: SAR[3] wind speeds from the Envisat satellite have been lifted to 100 m, using temperature and heat flux (which determine stability) from a numerical weather forecasting model (WRF[4]), but the results underestimated the measured wind speed even more than the WRF model wind speeds did. In the NORSEWInD project, wind mast and LIDAR data have been used to better understand wind profiles. Incorporating this new knowledge has led to better estimates of the 100 m wind speeds but the quality of the results is now limited by the quality of the planetary boundary layer height and the sea surface temperature in WRF.
- The OWA-NEEZ wind atlas is based on different versions of the Hirlam model. Earlier versions are in general less accurate than the later versions which may introduce changes in the wind which are not real. Because the atlas is not based on a homogeneous data set, it cannot be used to derive trends or make time-series.

So all existing wind atlases are based on measurements (except for the OWA-NEEZ wind atlas which is based on an inhomogeneous model data set) and periods that are not long enough to be sure that the long-term variability of the wind has been captured.

Based on the findings presented in this report, we recommend making a high resolution wind atlas for the North Sea that includes information on the long-term variability of the wind climate, provides information up to at least 200 m height and can reproduce more than just a climatological average of stability effects on the wind profile. In part 2 of this report we present a wind climatology which meets all these requirements. It is based on reanalyses model ERA-Interim (to ensure that long-term variability is included) and operational atmospheric weather forecasting model Harmonie (to enhance the resolution). At this stage it is no more (or less) than model climatology and validating against observations is still needed. Therefore validation will be the main recommendation for part 2 of this report.

[3] SAR: Synthetic Aperture Radar
[4] WRF: Weather Research and Forecasting model

Introduction

It is the Dutch government's target to realise 14% renewable energy in 2020 and 16% in 2023 (Energieakkoord voor duurzame groei SER 2013). To achieve this, the government intends to significantly increase wind energy production on land (to 6000 MW nominal capacity in 2020 which implies an increase of about 650 MW every year[5] and at sea to 4450 MW in 2023 which implies 3450 MW more than already planned). This is ambitious, especially for offshore wind energy production where this can only be accomplished in an economically viable way if production costs are reduced by 40% (conform the 2011 Green Deal Offshore Wind Energy between government and the Dutch Wind Energy Association NWEA representing the wind energy sector). In order to assess the wind power that will actually be produced if and when these nominal capacity targets are met, the government requires high quality wind climatology at or around hub height, especially at sea.

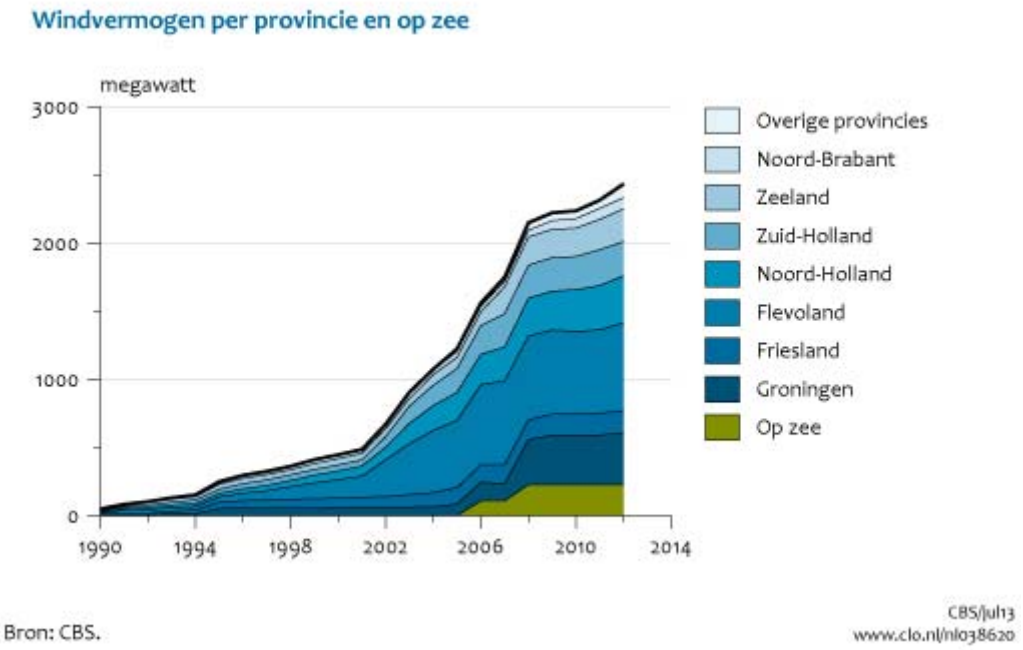

Figure 1.1 Dutch nominal capacity wind power 1990-2012 per region (blue) and offshore (green) (source: CBS)

There are two parts to this KNMI report on North Sea wind climatology. Part 1 gives an overview of the existing wind atlases and describes how they are made and what their limitations are and part 2 presents a wind climatology in which the best available stability estimates are incorporated in the wind profile at every grid box and point in time and the long-term variability of the wind climate is included.

[5] Document "Windparken op land" on site http://www.rijksoverheid.nl/onderwerpen/duurzame-energie/windenergie/windenergie-op-land (31-3-2014)

1 Existing Wind Atlases Onshore

An overview of the main onshore wind atlases that are used in the wind energy sector can be found on www.wind-energy-the-facts.org. This site shows the results of the WindFacts project which ran from November 2007 to October 2009 and was led by the EWEA (European Wind Energy Association).

1.1 The European Wind Atlas[6] at 50 m

The European Wind Atlas (published in 1989 for the Commission of the European Communities by Risø National Laboratory) is used extensively by developers and governments for estimating the size of the wind energy resource and regional variations (figure 1.1). In this map the influences of local topography have been removed and only the variations on the large scale are shown.

The European Wind Atlas uses 3 hourly meteorological data from a selection of monitoring stations. For The Netherlands wind measurements were used from 6 observation sites[7] (Eelde, Eindhoven, Leeuwarden, Schiphol, Terschelling and Texel Lichtschip) from 1970 up to and including 1976.

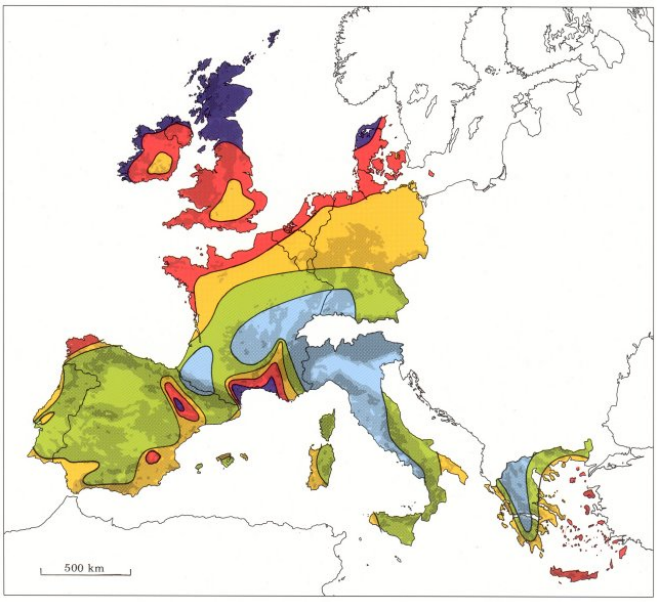

Wind resources[1] at 50 metres above ground level for five different topographic conditions

	Sheltered terrain[2]		Open plain[3]		At a sea coast[4]		Open sea[5]		Hills and ridges[6]	
	$m\,s^{-1}$	Wm^{-2}	$m\,s^{-1}$	Wm^{-2}	$m\,s^{-1}$	Wm^{-2}	$m\,s^{-1}$	Wm^{-2}	$m\,s^{-1}$	Wm^{-2}
	> 6.0	> 250	> 7.5	> 500	> 8.5	> 700	> 9.0	> 800	> 11.5	> 1800
	5.0-6.0	150-250	6.5-7.5	300-500	7.0-8.5	400-700	8.0-9.0	600-800	10.0-11.5	1200-1800
	4.5-5.0	100-150	5.5-6.5	200-300	6.0-7.0	250-400	7.0-8.0	400-600	8.5-10.0	700-1200
	3.5-4.5	50-100	4.5-5.5	100-200	5.0-6.0	150-250	5.5-7.0	200-400	7.0- 8.5	400- 700
	< 3.5	< 50	< 4.5	< 100	< 5.0	< 150	< 5.5	< 200	< 7.0	< 400

Figure 1.2 European Wind Atlas Onshore : the annual wind speeds and wind power resources at 50 m height above ground level estimated for 5 wind regions shown on the map and 5 topographic conditions in the table below the map (source: Risø National Laboratory, Denmark)

[6] http://www.windatlas.dk/Europe/Index.htm
[7] http://www.windatlas.dk/Europe/About.html: view the stations of the European Wind Atlas in Google Earth

The wind measurements, from sensors usually at 10 m above the surface, are vertically extrapolated using the integrated computer model WAsP (Wind Atlas and Application Program) with a number of submodels: the shelter model, the roughness change model, the stability model and the orographic model (figure 1.3 and 1.4) which are described in detail in Troen et al (1989). The vertically extrapolated measurements, for example at 50 m height as in figure 1.2, are horizontally interpolated so the map contours of equal wind speed can be drawn. How the interpolation was performed is not clear from the documentation but this is not so important because the map is mainly for general use and the real business of predicting the wind speed at potential sites of interest for producing wind power does not rely on the map but on the vertically extrapolated measurements of a nearby station (see section 1.1.1).

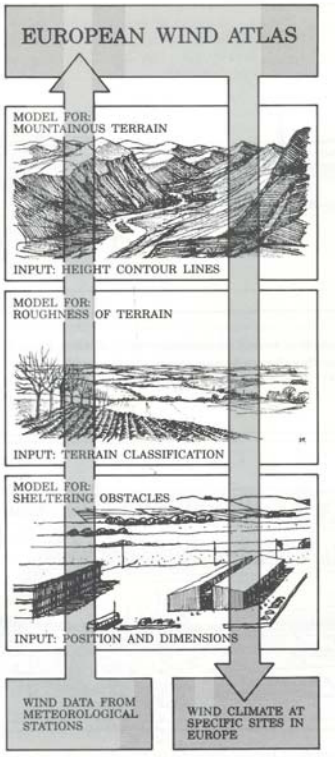

Figure 1.3 The WAsP methodology used to make the European Wind Atlas. The roughness change model, the shelter model and the orographic model are used to convert the raw wind measurements to regional wind climatologies (referred to as "European Wind Atlas" in the figure). In the reverse process, the wind climate at nearby sites with surrounding terrain similar to that of the measurement site can be estimated from the regional wind climatology.

1.1.1 WAsP

With the WAsP methodology detailed information about the wind climate from one location (the predictor site) can be transformed so that it is representative for another (the predicted site, where the wind turbine installation is planned). Two steps are distinguished (figure 1.3): first the observations are "cleaned", removing the effect of roughness, orography and sheltering obstacles at the predictor site ("way up" in figure 1.3) to produce a regional wind climate[8]. On the "way down" the wind climate of the predicted site is calculated using a model of the sheltering obstacles and roughness and orography corresponding to this site to modify the regional wind climate. The two sites should be within 100 km of each other and the terrain of both sites should be as similar as possible. Note that the regional wind climate is applied without any attempt to interpolate between the observation station locations.

For the calculation of the regional wind climate in the European Wind Atlas, measurements from and metadata about the observation site are used:

- Measurements from more than 200 observation sites are used which have been recorded every 3 hours for a period of 10 years. The measurements are analysed to produce the histograms (giving the frequency of occurrence of wind speeds in bins of 1 m/s and per wind direction sector of 30^0) which form the input to the model.
- Metadata include position and dimensions of nearby sheltering obstacles, terrain height, roughness length roses and terrain classification (e.g. in 4 terrain classes). The four terrain classes that are distinguished are: z_0 = 0.0002 m for water areas, z_0 = 0.03 m for open areas with few wind breaks; z_0= 0.10 m for farm land with wind breaks (the mean separation of which exceeds 1000 m) and some scattered built up areas and z_0= 0.40 m for urban districts and farm land with many wind breaks. In the current version of WAsP five terrain classes are distinguished (source: WAsP-support).

WAsP uses the metadata and the sub-models mentioned earlier (figure 1.3 and 1.4) to, first of all, transform the wind direction sector-wise histograms of wind speeds from each station to what would have been measured far upwind from the station before the obstacles, surface roughness and orography of the surroundings have affected the measurements. This transformation makes the wind representative for a wider area than the original measurements. The resulting histograms are referred to as 'corrected histograms' in figure 1.4. The correction factors used to calculate the corrected histograms are wind speed independent : for a given wind direction sector all the wind speed bins are transformed using the same factor.

[8] The term "regional" is only partly accurate because the wind climate is representative only for sites with surrounding terrain similar to that of the predictor site where the observations were made even if the predicted site is very close.

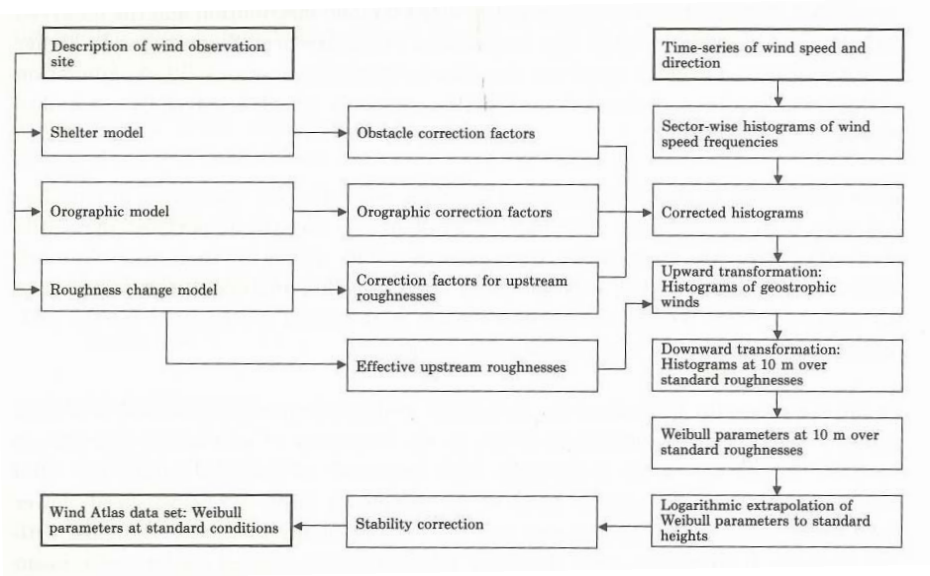

Figure 1.4 Schematic representation of the WAsP methodology used to make the regional wind climatologies, in the figure referred to as "Wind Atlas data set" (source: Troen, 1989)

The corrected histograms are then converted into histograms of the geostrophic wind using the geostrophic drag law (formula 1.1). This is the relation between the geostrophic wind (figure 1.5) and the surface friction velocity (measure of the surface stress; see formula 1.2). Non-neutral stability can be taken into account by making constants A and B in formula 1.1a dependent on stability parameter μ (formula 1.1c). However, the values of A and B used for the European wind atlases and the KEMA-SenterNovem wind atlas (section 1.2) seem to be the constant values for neutral stability since the stability correction is performed in the last step of figure 1.4. (see section 1.1.4)[9].

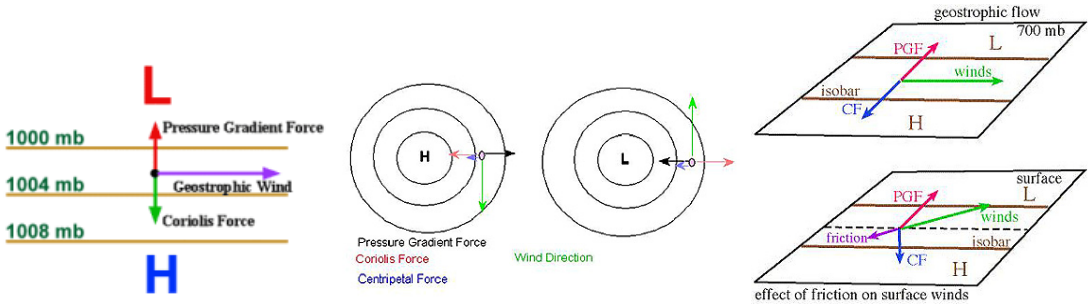

Figure 1.5 The geostrophic wind (left panel) is the component of the wind resulting from the pressure gradient and the Coriolis effect. When the isobars are curved, the centripetal force is also taken into account (middle panel). The geostrophic wind is a good approximation for the wind at higher levels, but the wind at lower levels depends on the ground friction too (right panel).

[9] For all but the last step in the Wind Atlas model (figure 1.4) Troen (1989) is not clear whether A and B are have the values for neutral stability or the climatological average stability (slightly different form neutral) . For the KEMA-SenterNovem wind atlas the same values of A and B are used as in the European Wind Atlas (Hans Cleijne, DNV GL, formerly KEMA): those representing the climatological average stability.

Instead of transforming all the data pairs (wind speed and direction) of the corrected histograms, the sides of the bins containing the data pairs are transformed. Formula 1.1a and 1.1b are used to transform respectively the two wind speeds and the two wind directions that define each bin. The number of data pairs in the original corrected histograms are the same as in the geostrophic histogram bins.

In formula 1.1 values of u_* and z_0 are needed to calculate the geostrophic wind speed. The friction velocity, u_*, can be calculated using formula 1.3 if u(z), z_0 and Monin-Obukhov length L, a measure for the stability, are known. In WAsP the roughness lengths (z_0) used for these two formulas are different. For the geostrophic wind the "effective surface roughness" is required which represents the cumulative effect of all the different surface roughnesses (out to about 10 km from the location of the wind mast) which affect the full extent of the PBL. For the friction velocity, the specific effect on the friction velocity of each successive upstream roughness (affecting successively higher parts of the wind profile) is calculated to obtain the upstream friction velocity. This is suitable (together with the effective surface roughness) for calculating the geostrophic wind speed at the very top of the wind profile.

The geostrophic wind histograms could have been used as a means of representation of the regional climatology, but instead the transformation process is continued with a downward transformation to 10 m for the four standard roughness lengths (z_0 = 0.0002 m, 0.03 m, 0.10 m and 0.40 m). For this downward transformation neutral stability (logarithmic wind profile) is assumed. This means that any undesirable deviation from the logarithmic wind profile due to stability effects in the upward transformation is to a large extent undone. For each 30^0 wind sector, the 10 m wind speed frequency distribution is fitted to a Weibull function to obtain the two Weibull parameters which describe the distribution adequately.

Then the Weibull parameters corresponding to the higher standard levels (25, 50, 100 and 200 m) are calculated by applying a climatological average[10] wind profile which differs from the logarithmic wind profile (assuming neutral stability) due to non-neutral stability effects. Two climatological average wind profiles are used: one for land and one for sea with coastal areas treated as a transition zone with a weighting based on distance to the sea. The climatological wind profiles are based on the deviations from the logarithmic profile caused by the variation of the surface heat flux quantified by the climatological average and root-mean-square (see section 1.1.4). Both the effect on the climatological average wind speed as on the standard deviation are determined and used to calculate Weibull parameters that describe wind speed frequency distributions consistent with the climatological effect of non-neutral stability.

[10] WAsP does not work with 10 min or hourly data but with the frequency distributions of the wind measurements so the Ψm-function can only be applied to the average wind profile (Cleijne, DNV GL, former KEMA).

The geostrophic drag law assumes a balance in the atmospheric boundary layer between the pressure gradient force (related to the change in surface air pressure with distance) and the frictional force at the earth's surface. This balance can theoretically be derived under idealised conditions of stationarity (no change in time), homogeneity (the roughness of the terrain and the density of the air is the same everywhere) and barotrophy (pressure gradient constant over the depth of the boundary layer so no vertical pressure gradient):

$$U_G = \frac{u_*}{\kappa}\sqrt{\left(\ln\frac{u_*}{f z_0} - A\right)^2 + B^2}$$

(geostrophic drag law) (1.1a)

$\sin \alpha = - (B u_*) / (\kappa U_G)$ (1.1b)

$\mu = (\kappa u_*) / (f L)$ (1.1c)

$\tau = \rho u_*^2$ (1.2)

$u(z) = [\ln(z/z_o) - \psi(z/L)] u_*/\kappa$ (Businger-Dyer formula) (1.3a)

(an alternative Businger-Dyer formula is used in the NORSEWInD project where u(z) also depends on the height of the Planetary Boundary Layer, formula 2.1e)

$L = (T_0 C_p u_*^3) / (\kappa g H_0)$ (Monin-Obukhov length) [11]
(1.3b)

- U_G = geostrophic wind
- u_* = friction velocity, related to the measured wind speed (u) at height z according to the Businger-Dyer formula (1.3a) where $\psi(z/L)$ is an empirical stability function which is 0 for a neutral atmosphere (see par 1.1.4 formula 1.6 and 1.10 to 1.12)
- κ = von Kármán constant (0.04)
- f = Coriolis parameter (value is determined solely by the latitude of the location)
- z_0 = surface roughness
- A and B: empirical constants (with values respectively of 1.8 and 4.5) in neutral conditions and dependent on stability parameter μ (1.1.c) when the atmosphere is (un)stable
- α = angle between the near surface winds and the geostrophic wind (the wind not only slows down as one nears the surface, the wind direction also backs, which means turns anti-clockwise looking down from above)
- τ = shear stress [N m^{-2}]
- ρ = air density which depends on temperature (1.2250 kg/m^{-3} at 15 ºC)
- T_0 and H_0 = surface absolute temperature and heat flux
- C_p = heat capacity of air at constant pressure
- g = acceleration of gravity (9.8 m/s^2)

[11] With this definition of the Monin-Obukhov length L, L < 0 indicates unstable and L > 0 stable (formula 1.6 for the stability function). In the Norsewind project an alternative definition for the Monin-Obukhov length is used with a minus sign (see formula 2.1c) so there L < 0 indicates stable and L > 0 unstable (formula 1.12 for the stability function)

This way 20 pairs of Weibull parameters (4 roughness classes x 5 heights) for each measurement location are constructed from which an onshore wind (energy) map and an offshore wind (energy) map can be derived. The onshore wind map represents five data sets for 5 terrain classes at 1 height (figure 1.2 , using 3 of the 4 roughness classes plus classes for coastal and hilly terrain) and the offshore wind map five: for 5 heights and 1 roughness class (figure 2.1).

Giebel en Gryning (2004) examined the limitations of using a climatological average of the stability effects on the wind profile by estimating the wind speed measurements around 100 m height from those near the surface at two high masts. Both are in open flat terrain, one on the west coast of Denmark and the other inland in the northeast of Germany. The greatest errors were found when the atmosphere was stable (mostly at night). At the inland site (part of) the surface layer up to 200 m was stable about half the time. Fortunately for WAsP the wind speed is low (6 m/s or less at 60 m height in Denmark) for about half of the stable cases which means that the error using a climatological average in terms of wind energy production will be low. The effect of the stable cases at higher wind speeds was not quantified but since this occurs 25% of the time, it is probably important. Other American and Danish studies (Rareshide et al, 2009; Wagner et al, 2009;Wharton and Lundquist 2011) have quantified the effect but the results vary wildly from a 20% decrease of wind power to a 20% increase in very stable conditions compared to neutral stability. The effect varies so much because it depends on the interplay between the height of the wind turbine and the local stability-related meteorological conditions. Wharton (2012) found that there is an opposite effect on wind power production for stable and unstable conditions, so it is possible that both effects cancel each other over a longer period. Evidently, more research is required to evaluate the effect of stability on wind power production.

1.1.2 Shelter model in WAsP

Close to an obstacle such as a building the wind is strongly influenced by the presence of obstacles. The effect extends vertically to about 3 times the height of the obstacle and downstream to about 30 to 40 times the height. For points of interest within this zone, the sheltering effect on the wind speed is taken into account (wind direction stays the same in the model). However, the effect in the immediate wake of the obstacle, is not modelled correctly. The immediate wake extends downstream by 5 object heights and reaches a height of twice the object height.

1.1.3 Roughness change (or internal boundary layer) model in WAsP

There are different ways to describe the planetary boundary layer (PBL). One way is to divide the PBL in two layers which are described with two different formulas (the so called two layer conceptual model of the PBL: 2LM). In the 2LM method a distinction is made between the local roughness which affects the lower layer of the PBL and the regional roughness which affects the upper layer. Another method, which is used in WAsP, is based on the same formulas as the 2LM but the roughness input for the formulas is more detailed. In WAsP, a roughness change or internal boundary layer (IBL) model is used to model the effect of roughness (change) on the wind speed in the IBL. Each roughness change creates another IBL at the surface,

which increases in depth the further away you get from the roughness change. Verkaik (2003) found that 2LM handles highly heterogeneous regions (e.g. coastal areas) better than IBL models.

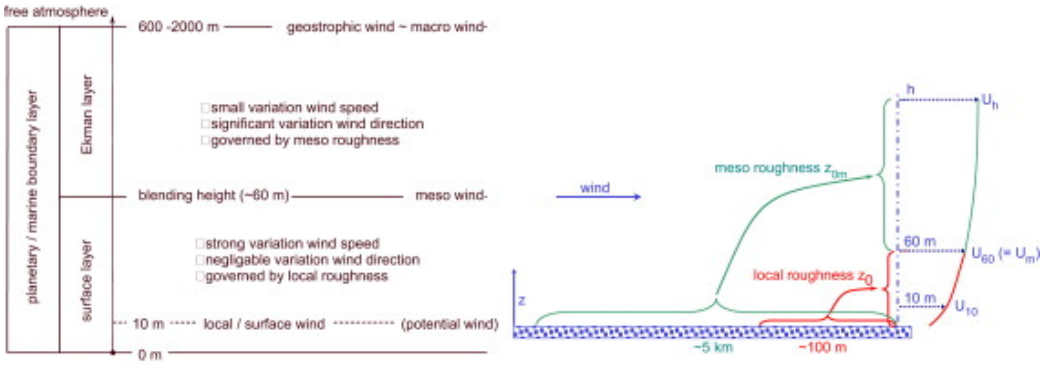

Figure 1.6 Left panel : schematic diagram of the properties of the wind in the two-layer modelof the PBL. Right panel : relation between surface roughness and the wind speed profile, for these two layers (source: Caires, 2012)

The two layer conceptual model of the planetary boundary layer is shown schematically in figure 1.6 and described in more detail in the following text. Small-scale changes in surface roughness (e.g. some trees in a field) affect the wind from the surface up to 60 m height if these changes occur up to 2 km from the point of interest (the effect is largest for changes at 600 m). Larger changes (e.g. a forest edge) affect the wind all the way to the top of the PBL, at least if these changes are within 9 km from the point of interest (the effect is largest for changes at 3 km). In figure 1.6 these horizontal distances are summarised respectively as "~100 m" and "~5 km". Because the PBL can in this way be seen as 2 layers that are fundamentally different (a surface layer up to about 60 m and an Ekman layer from about 60 m to the top of the PBL), we distinguish between the local roughness (z_{0l}) and the regional or meso roughness (z_{0m}). The model can be applied separately to each wind direction at the point of interest. In the Ekman layer the geostrophic drag law (formula 1.1) applies and in the surface layer the Businger-Dyer formula (formula 1.3) for neutral stability. The two layers are made to match at 60 m height by assuming that the friction velocity is the same in both equations at that height, despite the fact that the formula's use two different roughness lengths.

In WAsP a different but similar model of the PBL has been used: the roughness change or internal boundary layer model. The Businger-Dyer formula, assuming neutral stability, is still used to describe the wind profile but the surface roughness is analysed in more detail. In this model an internal boundary layer (IBL) develops downwind from each roughness change (and accompanying change in surface friction velocity). At a certain distance x downwind from the roughness change the IBL has grown to a height h (approximately equal to one tenth of x, but this varies a little depending on the roughness). By making (the right hand side of) the Businger-Dyer formula for u(h) with the upwind roughness in the formula equal to the same formula but then with the downwind roughness, one finds that the relationship between the upwind and downwind friction velocity depends only on the two roughnesses. By applying the IBL model to the succession of roughness changes moving away from the observation site, the friction velocity far upwind can be

obtained knowing the wind speed measured at the site, the height of the sensor and the surface roughness lengths. The wind profile of the IBL and the method used to "average" the succession of surface roughness lengths to obtain one effective surface roughness length for the whole of the PBL are described in detail in the blue panel below. With this effective roughness length and the friction velocity at 10 km upstream from the wind mast, the upstream wind speed (free of the effects of the roughness within 10 km of the mast) can be calculated. The geostrophic wind speed can now also be calculated using the friction velocity at 10 km from the wind mast and the effective surface roughness for the whole 10 km distance. In this way the "corrected histograms" and the "histograms of geostrophic winds" of figure 1.4 can be produced.

The wind profile in the IBL and the effective surface roughness of the PBL

The wind profile below h in the IBL has changed by partially adapting to the downwind surface conditions; below 0.09h the wind profile is assumed to be fully adapted to the downwind roughness. Above 0.3h the wind profile is still determined by the upwind roughness and between these heights lies a transition layer.

An effective surface roughness for the whole of the PBL does not follow directly from the succession of IBLs because it produces results that do not conform to the geostrophic drag law. This is due to the roughnesses far from the wind mast affecting the wind profile in the IBL model just as much as closer roughnesses. A weighting factor is therefore applied to exponentially reduce the effect of the roughness changes so that at 10 km distance from the wind mast a roughness change has no effect on the wind profile. The way the weighting factor is implemented also results in roughnesses that are a function of the roughnesses nearer the mast with the roughnesses nearer the mast having the highest weighting. This produces what is referred to as the "effective surface roughness" which is a weighted average of the roughnesses out to 10 km. The assumption here is that the surface roughness further than 10 km from the wind mast no longer affects the geostrophic wind speed above the mast.

For the observation sites roughness lengths are given for each wind direction sector (of 30°, see figure 1.7) out to the distance (10 km) where roughness no longer has an effect on the wind profile. If the roughness length of a given sector changes with distance to the observation site, the distance to and magnitude of this change is also given for up to 15 changes.

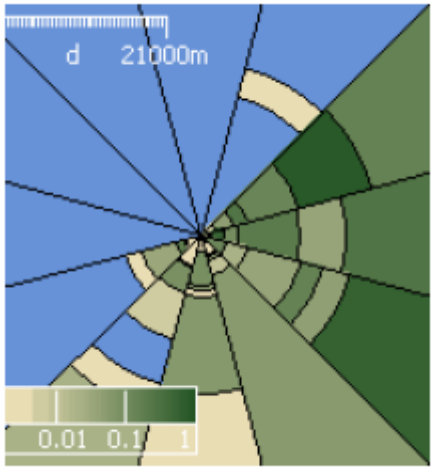

Figure 1.7 Example of a WAsP roughness rose for coastal site, Hook of Holland

The roughness lengths and distances to the changes in roughness are based on 'paper' topographical maps for each country, mostly from national survey agencies. The analysis was usually conducted out to about 10 km from the observation site, but it was more detailed close to the site to describe the IBL at the relatively low height of the wind sensors correctly. The paper maps date from 1970 to 1976. Satellite-based digital land-use maps were not available in those days. The empirical formula of Lettau (1969) is used to estimate the roughness length of groups of obstacles more than 30-40 times the height of the obstacle away from the site (the shelter model of section 1.1.4 accounts for part of the wake of closer obstacles). The formula takes into account the height of the roughness element (obstacle), its cross section facing the wind and the average horizontal area available to each roughness element. Corrections are applied to account for the porosity of the element and the lifting of the air flow over closely packed obstacles (e.g. a forest).

The roughness length found for land stations in the Netherlands is mostly 0.01 m which is according to Troen et al (1989) conform the value for airport runway areas and mown grass. For water areas a roughness length of 0.0002 m is used. Troen et al (1989) concluded that for the moderate to high winds of interest (around 10 m/s at 10 m above mean sea level) 'a fixed value of 0.0002 m gave results as good as the Charnock[12] formula' with a Charnock factor of 0.014.

Much research has been done on how to parameterise the drag coefficient in weather forecasting models. Figure 1.8 (Baas, 2014) illustrates that drag relations in modern atmospheric weather models are not described by a Charnock formula with one Charnock factor for all wind speeds: the model values (black) do not follow the Charnock formula (red lines) for the whole wind spectrum. In Harmonie e.g. (KNMI's new high resolution atmospheric forecasting model on a 2.5 km grid) the drag coefficient becomes constant for wind speeds above 20 m/s (ECUME drag formulation, Weill et al, 2003) and in ERA-Interim the Charnock factor is not a constant, but a function of the sea state (Bidlot et al, 2007).

[12] Charnock's model (1955) relates the roughness length to the friction velocity. The Charnock constant in the formula is site specific and often assumed to be 0.032 for The North Sea and 0.018 for Lake IJssel.

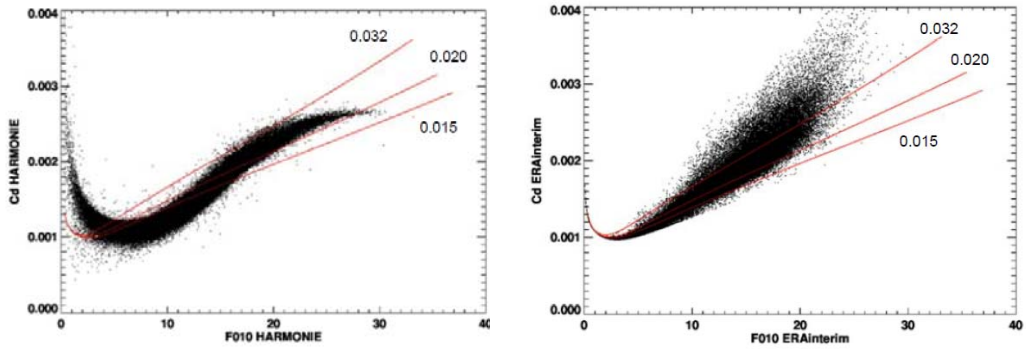

Figure 1.8: Left panel: The Harmonie drag relation over sea for the 17 storms analysed in the SBW-wind project. The solid lines show the Charnock relation with Charnock constants of 0.015, 0.020 and 0.032 and support Troen's choice of 0.014 for speeds around 10 m/s. Right panel: The ERA-Interim drag relation over sea for the same 17 storms demonstrating that older models give poorer results. (source: Baas, 2014).

1.1.4 Stability model in WAsP

Stability modifications to the logarithmic wind profile are based on the climatological average and root-mean-square (rms) of the surface heat flux. The following values are used for all analysed stations:

- average heat flux over land (dH in formula 1.4): -40 Wm^{-2}
- average heat flux over sea (dH in formula 1.4): 15 Wm^{-2}
- rms heat flux over land: 100 Wm^{-2}
- rms heat flux over sea: 30 Wm^{-2}

To describe the climatological average wind profile (formula 1.9) a set of formulas need to be derived (formula 1.4 to 1.8). The derivation is summarised in the blue panel below.

Derivation of the climatological average wind profile

First we have to derive a formula for the offset from the neutral value of u_* (du_*). This formula (1.4) is derived from the differential form of the geostrophic drag law (formula 1.1a) where the dependence on the surface heat flux is introduced via A and B being functions of the stability parameter μ (formula 1.1c and 1.3b). The differential form makes it possible to evaluate the differences between the climatological average wind profile and the logarithmic profile caused by non-neutral stability when we assume that the differences are small. The differential form is first used to evaluate the offset from the neutral value of u_* (du_*) by inserting the climatological mean value of the surface heat flux into dH. When the rms of the heat flux is inserted into dH, du_* then gives the rms of fluctuations of u*.

$$du_*/u_* \approx [\, cg / (f T_0 C_p \rho U_G^2) \,]\, dH \qquad (1.4)$$

- u_* = friction velocity, related to the measured wind speed at height z according to the Businger-Dyer formula (1.3a, which describes the vertical wind profile) where $\psi(z/L)$ is an empirical function which is 0 for a neutral atmosphere (see par 1.1.4 formula 1.6 and 1.10 to 1.12)
- $c \approx 2.5$
- g = acceleration of gravity (9.8 m/s^2)

- f = Coriolis parameter depending on latitude
- T_0 = surface absolute temperature
- C_p = heat capacity of air at constant pressure
- ρ = air density
- U_G = geostrophic wind
- dH = climatological mean value of the surface heat flux

In deriving formula 1.4 small quantities are ignored and the following are assumed constant:
- z_o, f and U_G are constant
- A and B (functions of the stability parameter μ) take the following values in neutral stability (where μ = 0 because L tends to infinity) : $A(0) \approx 1.8$, $B(0) \approx 4.5$, $dA/d\mu \approx -0.2$, $dB/d\mu \approx +0.2$.

Formula 1.5b is derived from the differential form (1.5a) of the Businger-Dyer formula (1.3a which describes the wind profile). The dependence on the surface heat flux is again introduced via the Monin-Obukhov length (formula 1.3b). Formula 1.4 and the same constants as before are assumed to apply. At a certain height the offset of the wind speed from the logarithmic wind profile caused by the surface heat flux is minimal and if we call this height z_m then $du(z_m) \approx 0$ and the differentials disappear from the differential form of the Businger-Dyer formula.

$$du(z) = [\ln (z/z_0) - \psi(z/L)\ ]\ du_*/\kappa \ - \ [u_*/\kappa \ * d\psi/dL \ * dL/dH\ ]dH \qquad (1.5a)$$

$$\Delta u(z_m)/u_0(z_m) = \Delta u_* /u_{*0} - [\ \{\ \psi_m(z_m/L_{off}) \ + \psi_m(z_m/L_{rms})\ \}\ /\ \ln (z_m/z_0)\ ] \qquad (1.5b)$$

$$L_{rms} = F_{rms}\ \Delta H_{rms} \qquad (1.5c)$$

At the height of minimum variance z_m , the relative deviation from the neutral value of the mean wind speed $\Delta u(z_m)/u_0(z_m)$ is determined by the sum of the deviation caused by an average heat flux offset (ΔH_{off}) and a varying heat flux (ΔH_{rms}): formula 1.5b. This formula is derived by dividing the Businger-Dyer formula for $\Delta u(z)$ by the neutral stability form for $u_0(z)$. It is not obvious why an rms term should contribute to the relative deviation. It is required to correct for the asymmetrical form of the stability function (formula 1.6) which has a much stronger dependence on z on the stable side of neutral than on the unstable side. Without this term the relative deviation would produce an overestimation the wind speed at height z_m.

$$\Psi_m\ (z/L) = (1\text{-}16\ z/L)^{1/4} - 1 \qquad \text{(unstable conditions } z/L < 0) \qquad (1.6a)$$

$$\Psi_m\ (z/L) = -4.7\ z/L \qquad \text{(stable conditions } z/L > 0) \qquad (1.6b)$$

- z_m = height above the ground where the non-neutral stability deviation from the neutral wind profile is minimal
- $\Delta u\ (z_m)$ = deviation from the neutral value of the mean wind speed at height z_m
- $u_0\ (z_m)$ = neutral value of the mean wind speed at height z_m
- $\Delta u_* / u_{*0}$ = relative deviation from the neutral value of u_*
- $\psi_m(z/L)$ = function used in the Businger-Dyer formula (formula 1.3a) to describe modification of the neutral logarithmic wind profile due to (un)stability of the atmosphere
- L_{off} = Monin-Obukhov length (formula 1.3b) corresponding to ΔH_{off}
- ΔH_{off} = average heat flux offset
- L_{rms} = Monin-Obukhov length (formula 1.3b) corresponding to ΔH_{rms}
- F_{rms} = form factor that accounts for the fact that because of the difference in the form of the ψ-function from stable to unstable conditions, there will be a bias

toward higher values of wind speed at the height z_m

- z_0 = effective surface roughness

The next step is to derive the formula for z_m. By substituting the simplified neutral drag law (formula 1.7) into the differential form of the Businger-Dyer formula (formula 1.5a) a formula for z_m is obtained (formula 1.8).

$u_{*0} / G = 0.5 / \{\ln (Ro) - A(0)\}$ simplified neutral drag law (Jensen, 1964) (1.7)

$z_m/z_o \approx \alpha \, Ro^{\beta}$ (1.8a)

$Ro = U_G / (f z_o)$ (surface Rossby number) (1.8b)

- z_m = height above the ground where the climatological deviation from the neutral wind profile caused by non-neutral stability is minimal. Note that the height z_m is constant over large areas because of the weak dependency on z_0 ($\sim z_0^{0.1}$), except for coastal areas where z_m over sea is found to be roughly half of the over land value. At the Dutch inland observation station Cabauw z_m is about 100m.
- z_0 = effective surface roughness
- $\alpha = 0.002$
- $\beta = 0.9$
- U_G = geostrophic wind
- f = Coriolis parameter depending only on latitude

The relative deviation at height z_m evaluated using formula 1.5b is then adjusted for other heights using a profile function (formula 1.9c) to obtain the logarithmic wind profile adjusted for climatological average stability (formula 1.9a). The relative deviation of the friction velocity from it's neutral stability value is evaluated using formula 1.4 and is applied in formula's 1.9a and 1.9b to quantify the deviation this produces in the wind speed. Formula 1.9b is constructed in a similar way to obtain the profile of the standard deviation of the wind speed which takes into account the climatological average of the effects of stability.

$u(z) = u_0(z) \left[1 + \Delta u_{*off}/u_{*0} + (1 - f(z)) \, \Delta u(z_m)/u_0(z_m) \right]$ (1.9a)

$\sigma_u(z) = \sigma_{u0}(z) \left[1 + \Delta u_{*off}/u_{*0} \, |f(z)| \right]$ (1.9b)

$f(z) = 1 - \left[\ln(z_m/z_0)/\ln (z/z_0) \right] z/z_m$ (1.9c)

- $\Delta u_{*off}/u_{*0}$ = the relative deviation of the friction velocity u_* from it's neutral stability value (evaluated using formula 1.4)
- $\Delta u(z_m)/u_0(z_m)$ = relative deviation from neutral value of u at the height of minimum deviation, z_m (calculated using formula 1.8)
- f(z) is the profile function which describes the change with height of the deviations evaluated at height z_m
- z_0 = effective surface roughness

Formula 1.9 is used in the Wind Atlas model to calculate the degree of "contamination" by stability effects in the input data and to re-introduce proper values of contamination when calculating conditions at different heights and surface conditions, which is the last step of the model (see figure 1.4). This is particularly relevant if a land data-set is used to estimate

offshore conditions or the other way around because the contaminations are different due to different average heat fluxes. In this respect coastal areas are treated as intermediate zones where stability corrections for land and sea are applied with a weighting factor depending on the distance to the coast in the upwind direction and the width of coastal zone (assumed to be 10 km).

The description of the Ψ_m-function used here (formula 1.6) dates from 1964 (Jensen et al). Since then better versions of the Ψ_m-function have been developed. Beljaars and Holtslag (1991) refer to a review by Högström (1988) where several formulas for Ψ_m were compared to each other and to measurements (with z/L in the range from -3 to +1). Högström found that the then most widely used formulas for Ψ_m for unstable conditions (z/L < 0; Businger (1971) and Dyer (1974)) agreed with each other within ± 10% and with Högström's measurements. He also found a good match between most measurements and the formula ψ_m = -5z/L for stable conditions with z/L between 0 and 1. In 1984 Holtslag analysed stable Cabauw data up to z/L ≈ 10 and came up with an alternative formula for ψ_m (z/L), which was moderated in 1991 (formula 1.11 Beljaars/Holtslag) and appears to perform better than Businger's (Sharan et al, 2003; see also figure 1.9). The formula for ψ_m (z/L) used in the NORSEWInD project (section 2.3) is different again, but not only the Ψ_m-function is different: for stable conditions the Businger-Dyer formula (1.3a) is adapted so that it takes the height of the PBL into account (formula 2.1e).

Jensen (1964):

$\Psi_m (z/L) = (1\text{-}16\ z/L)^{1/4} - 1$ (unstable conditions $z/L \leq 0$) (1.6a)

$\Psi_m (z/L) = -4.7\ z/L$ (stable conditions $z/L > 0$) (1.6b)

Businger (1971)/ Dyer (1974):

$\psi_m = 2\ln [(1+x) /2] + \ln [(1+x^2)/2] - 2 \tan^{-1} (x) + \pi/2$

(unstable conditions $z/L \leq 0$) (1.10a)

where $x = (1 - 16\ z/L)^{1/4}$

$\psi_m = -5z/L$ (stable conditions $z/L > 0$) (1.10b)

Beljaars/Holtslag (1991):

$- \psi_m = a\ z/L + b\ (z/L - c/d)^{-d\ z/L} + bc/d$ (stable conditions $z/L > 0$) (1.11)

- a = 0.7
- b = 0.75
- c = 5
- d = 0.35

- z/L small: ψ_m behaves like $\psi_m = -5\ z/L$ (= Businger-Dyer)
- z/L large: $-\psi_m \approx a\ z/L$

NORSEWInD (2012):

$\psi_m = 3/2 \ln [(1 + x + x^2) / 3] - \sqrt{3} \arctan [(2x+1) / \sqrt{3}] + \pi / \sqrt{3}$

where $x = [1 - 12 (z / L)]^{1/3}$ (unstable conditions $z/L \leq 0$) (1.12a)

$\Psi_m (z/L) = -4.7\ z/L$ (stable conditions $z/L > 0$) (1.12b)

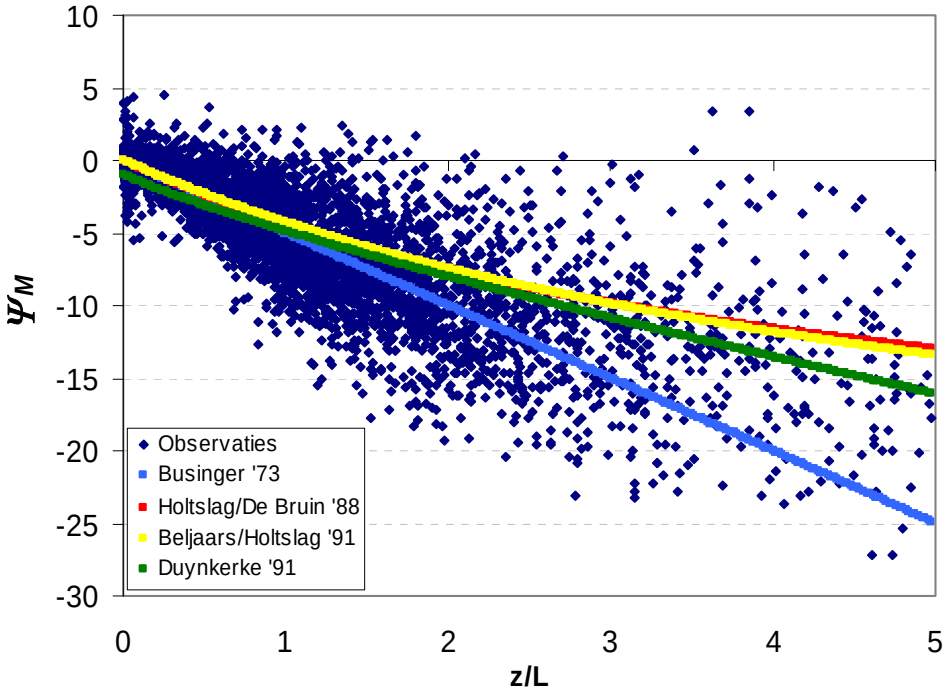

Figure 1.9 Different Ψ-functions for stable conditions compared to observations at Cabauw showing the improvements made since Businger (source: Baas KNMI)

1.1.5 The orographic model in WAsP

The orographic model is used to correct measured wind data for the effect of differences in terrain height around meteorological stations with the emphasis on terrain undulations with horizontal scales up to several tens of kilometres. Orographic

effects play a minor role in the Netherlands and are irrelevant at sea and are therefore not discussed in detail in this report. More information can be found in Troen et al (1989).

1.1.6 Verification of the European Wind Atlas

In Troen et al (1989) score schemes are presented, e.g. for the six Dutch land stations (figure 1.10). In the score schemes the names of the predicted stations are printed in full and the names of the predicting stations are abbreviated. So the WAsP-procedure shown in figure 1.3 gives a mean wind speed at Eelde of 4.4 m/s based on the observations at Schiphol, whereas in reality it was 4.5 m/s (in bold).

	Sch	Ein	Lee	Tex	Eel	Ter
Schiphol	**5.0**	4.7	5.2	5.1	5.1	5.5
Eindhoven	4.7	**4.4**	4.9	4.8	4.8	5.2
Leeuwarden	5.0	4.7	**5.1**	5.0	5.1	5.4
Texel Lichtschip	7.6	7.2	7.9	**7.6**	7.8	8.3
Eelde	4.4	4.2	4.6	4.5	**4.5**	4.9
Terschelling	6.9	6.6	7.2	6.9	7.1	**7.6**

Figure 1.10 Comparison of the WAsP method at 6 Dutch stations. Except for the inland station, Eindhoven and the station on the North Sea island of Terschelling, the predicted mean wind speeds compare well to the measured speeds. The other stations are representative of the near North Sea coast conditions so it is clear why Eindhoven is difficult to predict (source: Troen, 1989).

The wind atlas data have also been validated against six meteorological masts (the Ferrel mast in Portugal, the Kivenlathi mast in Finland, the Näsudden mast in Sweden, the Risø and Sprongø masts in Denmark and the Cabauw mast in the Netherlands). The measurements from the lowest sensors were used to predict the measurements made higher on the mast. For the Cabauw mast only one wind frequency distribution was available for all wind sectors combined (azimuth independent) and no detailed analysis of the surface roughness was performed. The results of two surface roughness assignments are given in figure 1.11 and they are worse than for the other masts where more detailed wind speed distributions were available and surface roughness analyses were made.

Height	Measured			Predicted					
				z_0 = 5 cm			z_0 = 15 cm		
z	A	k	E	A	k	E	A	k	E
10 m	4.7	1.79	97	4.7	1.79	98	4.7	1.78	98
40 m	6.5	2.09	218	6.6	1.99	235	6.4	2.06	204
80 m	8.0	2.52	343	7.8	2.19	352	7.5	2.25	312
120 m	9.0	2.47	487	8.6	2.23	473	8.4	2.27	435
200 m	9.9	2.28	698	9.9	2.18	727	9.9	2.21	709

Figure 1.11 Cabauw data are given in the form of a frequency table covering one year 1978/79. E is the wind power density in watts per square metre of wind turbine rotor area and A and k are the Weibull parameters. Results for two different surface roughness assignments are given, the higher one being the more realistic (source: Troen, 1989)

1.2 KEMA/SenterNovem Wind Atlas[13] at 100 m height

National wind atlases are also available with a higher resolution, based on a higher density of observation stations and using more detailed topographical information. An example of a national wind atlas is the KEMA/SenterNovem Wind Atlas at 100 m above the Netherlands (figure 1.12). This map was produced in 2005 and is based on 20 years of potential wind[14] observations (1983-2002) from 26 Dutch observation sites, which is significantly more than the 6 observation sites used for the European Wind Atlas mentioned earlier.

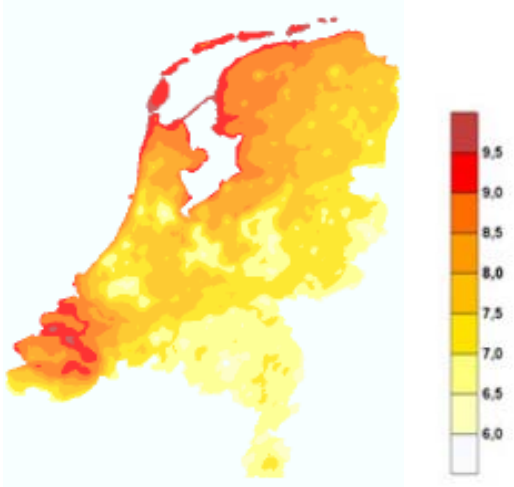

Figure 1.12 KEMA/SenterNovem Wind Atlas at 100 m for The Netherlands (legend shows wind speed in m/s).

[13] http://www.agentschapnl.nl/sites/default/files/2013/09/Windkaart%20van%20Nederland%20op%20100m%20hoogte.pdf
[14] Potential wind is a wind observation corrected for differences in measuring height (from 10 m), local roughness in the upstream sector (from the reference local roughness of 3 cm over land and 2 mm over sea) and in measurement methods: http://www.knmi.nl/klimatologie/onderzoeksgegevens/potentiele_wind/explanation.html

For the KEMA/SenterNovem Wind Atlas a 200x200 m surface roughness map was used. This roughness map was made with the LGN3+ land use map from Alterra and the WAsP-map program developed by KNMI. LGN3+ is based on satellite images from 1995-1997 and gives the roughness length for the Netherlands in 25 by 25 km grid boxes based on a table of 40 land use types. The information is 2 dimensional so, for example, the height of forests is not considered. The WAsP-map program is used to convert the LGN3+ roughness to 200 by 200 m grid boxes by averaging the drag coefficient at 10 m height. The influence of certain types of obstacles (3 dimensional) is underestimated because the horizontal dimensions are small while their height makes them important (figure 1.13).

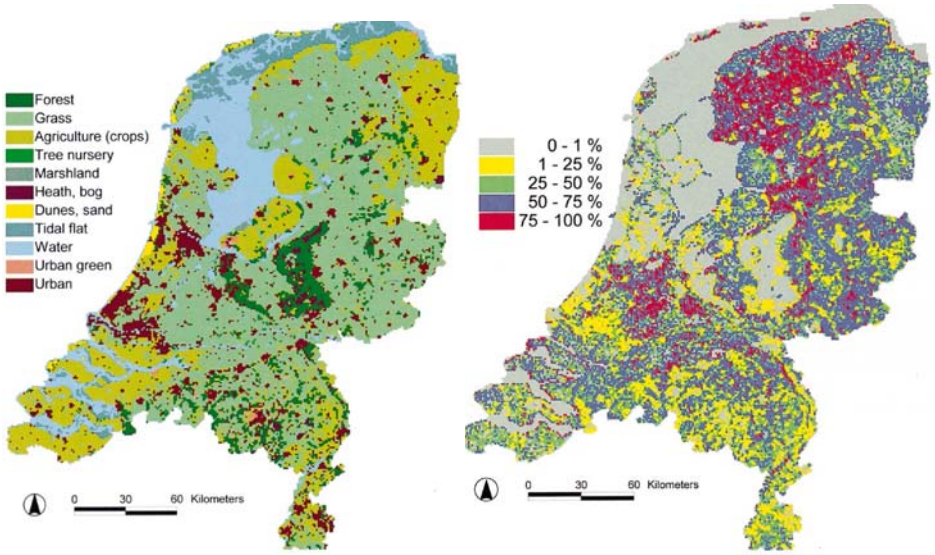

Figure 1.13 Underestimation of the effective roughness length (in %) as a result of lines of trees or dikes. For this work 1 by 1 km land use map LKN from 1997 was used and an extra drag coefficient was applied depending on the shape, height and the distance between the obstacles (source: De Jong, 1998)

For the conversion of the observations made at 10 m above the ground to 100 m the KEMA/SenterNovem Wind Atlas assumes a neutral atmosphere (logarithmic wind profile) with a correction based on the annual average atmospheric stability at the Cabauw wind mast (central part of the Netherlands). This is a simplification because in reality the atmosphere is more stable inland than on the coast.

Even more detailed maps were produced by KEMA/SenterNovem (figure 1.14).

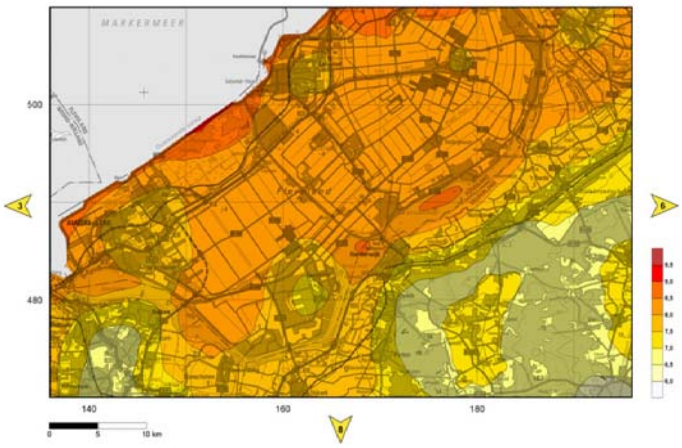

Figure 1.14 Example of a detailed KEMA/SenterNovem wind map (legend shows wind speed in m/s). (source: Windkaart van Nederland op 100 m hoogte, 2005)

2 Existing Wind Atlases Offshore

2.1 The European Wind Atlas[15] at 5 different heights above sea level

For the European offshore Wind Atlas wind measurements were used from 1970 to and including 1976 and from only a few observation sites on the North Sea (light ship Horns Rev Fyrskib in the German Bight and Texel Lichtschip just off shore Texel)[16].

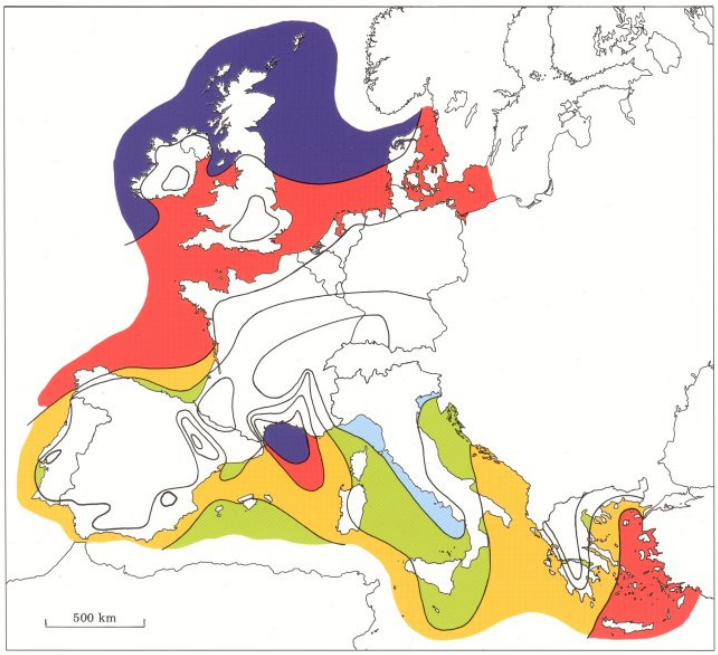

Wind resources over open sea (more than 10 km offshore) for five standard heights

	10 m		25 m		50 m		100 m		200 m	
	$m\,s^{-1}$	Wm^{-2}	$m\,s^{-1}$	Wm^{-2}	$m\,s^{-1}$	Wm^{-2}	$m\,s^{-1}$	Wm^{-2}	$m\,s^{-1}$	Wm^{-2}
	> 8.0	> 600	> 8.5	> 700	> 9.0	> 800	> 10.0	> 1100	> 11.0	> 1500
	7.0-8.0	350-600	7.5-8.5	450-700	8.0-9.0	600-800	8.5-10.0	650-1100	9.5-11.0	900-1500
	6.0-7.0	250-300	6.5-7.5	300-450	7.0-8.0	400-600	7.5- 8.5	450- 650	8.0- 9.5	600- 900
	4.5-6.0	100-250	5.0-6.5	150-300	5.5-7.0	200-400	6.0- 7.5	250- 450	6.5- 8.0	300- 600
	< 4.5	< 100	< 5.0	< 150	< 5.5	< 200	< 6.0	< 250	< 6.5	< 300

Figure 2.1 European Wind Atlas Offshore : the wind speeds at 50 m height above ground level (a.g.l) within the wind speed regions identified may be estimated for different topographic conditions using the table below the figure (source: Risø National Laboratory, Denmark)

In Troen et al (1989) score schemes are presented, e.g. for five North Sea stations and one land station: the two German Islands Helgoland and List/Sylt, the Dutch Island Terschelling, the two light ships Texel and Hors Rev and Skrydstrup Airport in southern Jylland. In the score schemes the names of the predicted stations are printed in full and the names of the predicting stations are abbreviated. So the WAsP-procedure shown in figure 1.3 gives based on the observations at Texel Lichtschip, a mean wind speed at Terschelling of 6.9 m/s, whereas in reality it was 7.6 m/s (in bold).

[15] http://www.windatlas.dk/Europe/oceanmap.html
[16] http://www.windatlas.dk/Europe/About.html: view the stations of the European Wind Atlas in Google Earth

	Hel	Lis	Tex	Hor	Skr	Ter
Helgoland	**7.2**	7.5	7.1	7.3	7.5	7.7
List/Sylt	6.8	**7.0**	6.7	6.9	7.0	7.3
Texel Lichtschip	7.7	8.1	**7.6**	7.8	8.0	8.3
Horns Rev Fyrskib	7.7	8.1	7.6	**7.8**	8.0	8.3
Skrydstrup	4.4	4.7	4.4	4.5	**4.6**	4.8
Terschelling	7.1	7.5	6.9	7.2	7.4	**7.6**

Figure 2.2 Comparison of five North Sea stations and one land station : the two German Islands Helgoland and List/Sylt, the Dutch Island Terschelling, the two light ships Texel and Hors Rev and Skrydstrup Airport in southern Jylland. Except for Terschelling, the comparisons are rather good. Skrydstrup which has a much lower mean value than the rest of the stations, is both well predicted and predicts well (source: Troen, 1989).

No off-shore meteorological masts were used to validate the wind atlas data.

2.2 OWA-NEEZ

The Offshore Wind Atlas of the Netherlands' Exclusive Economic Zone[17] (OWA-NEEZ) was published by ECN in 2011 and is based on 6 years of data from the numerical weather prediction model Hirlam. The atlas contains distributions of mean wind speed, Weibull parameters and reference wind speed in the Netherlands' Exclusive Economic Zone at 40, 90 and 140 meter above mean sea level. There are two versions of this atlas. In the version that was published in 2005, the sea surface roughness only depended on wind speed (Charnock relation), but in the 2011 version the sea surface roughness is a function of wave steepness too. The accuracy of the Weibull shape parameter was only improved by 1% - 2%.

The maps are based on time series (+00 until +06 hours) from subsequent Hirlam runs in the period 2003-2009. The disadvantage of the method is that different versions of the Hirlam model are used: the atlas is not based on a homogeneous data set. Wind and potential temperature are vertically interpolated between model levels assuming a Beljaars-Holtslag profile (in very stable conditions; formula 1.11 in section 1.1.4) or a Businger-Dyer profile (all other conditions: formula 1.10a in section 1.1.4); a bi-linear interpolation is used in the horizontal, between Hirlam grid points). Measurements are only used to validate the map (figure 2.3).

[17] https://www.ecn.nl/publications/ECN-M--11-031

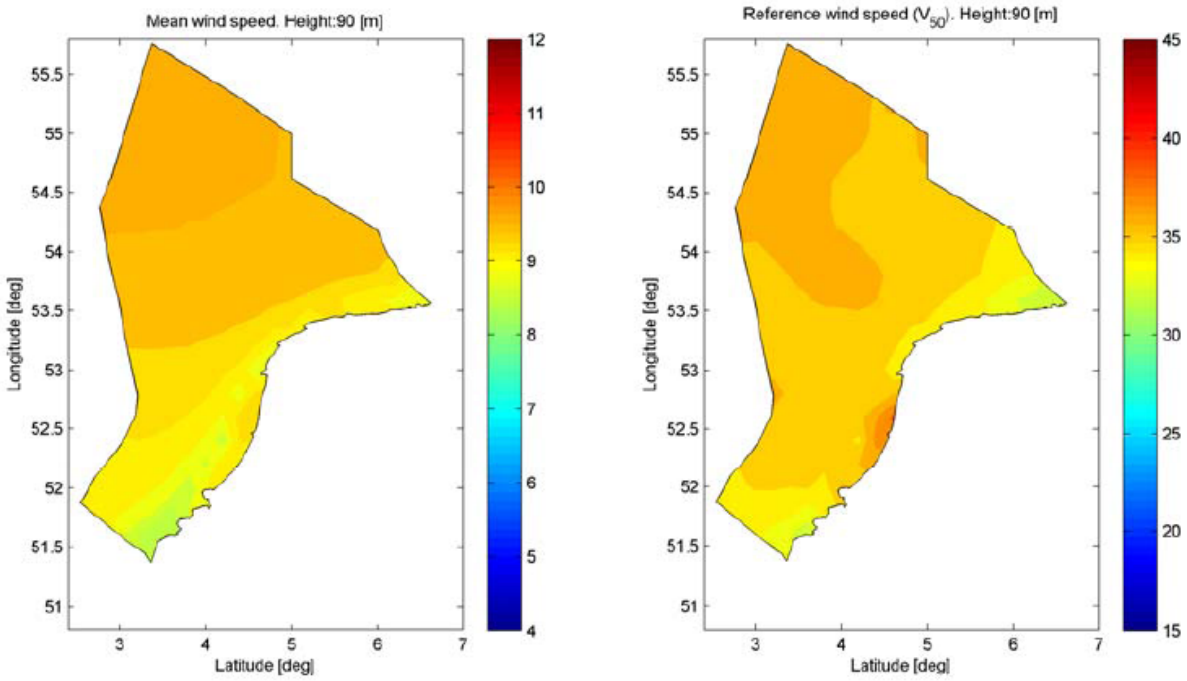

Figure 2.2a OWA-NEEZ mean wind speed and reference wind speed (which is the once in 50 year 10min extreme, calculated by using the Weibull parameters and the Gumbel-Bergstrom method) both at 90 m (source: Donkers, 2011).

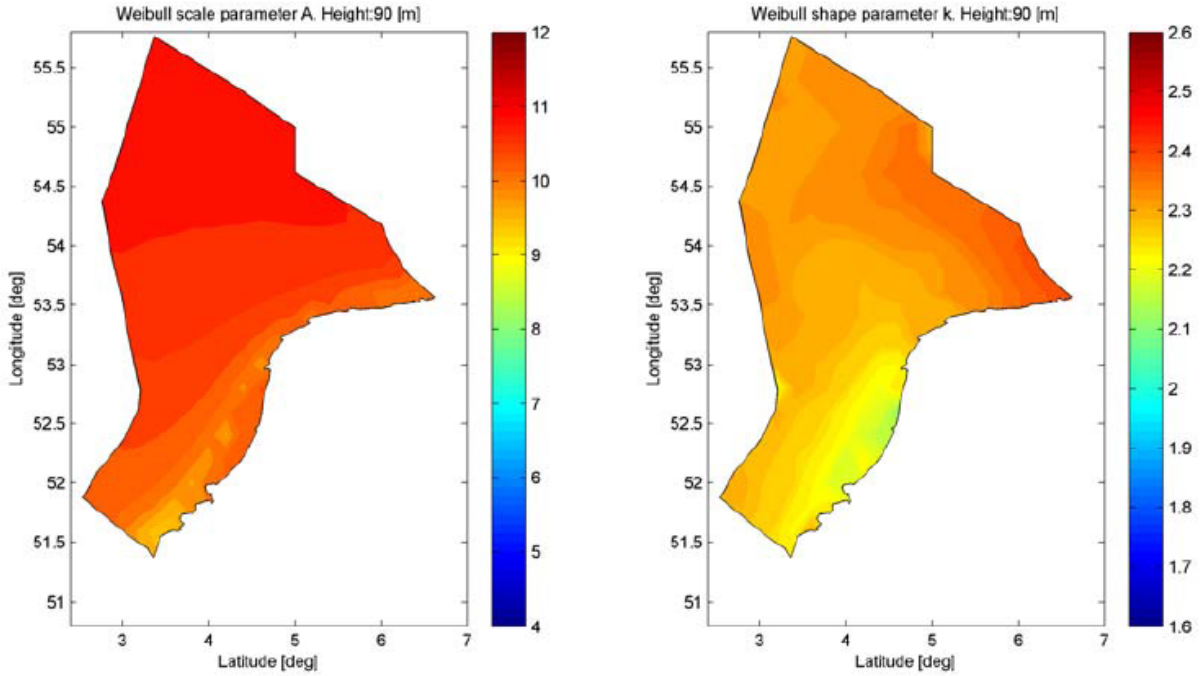

Figure 2.2b OWA-NEEZ Weibull scale parameter (left) and Weibull shape parameter (right) at 90 m (source: Donkers, 2011).

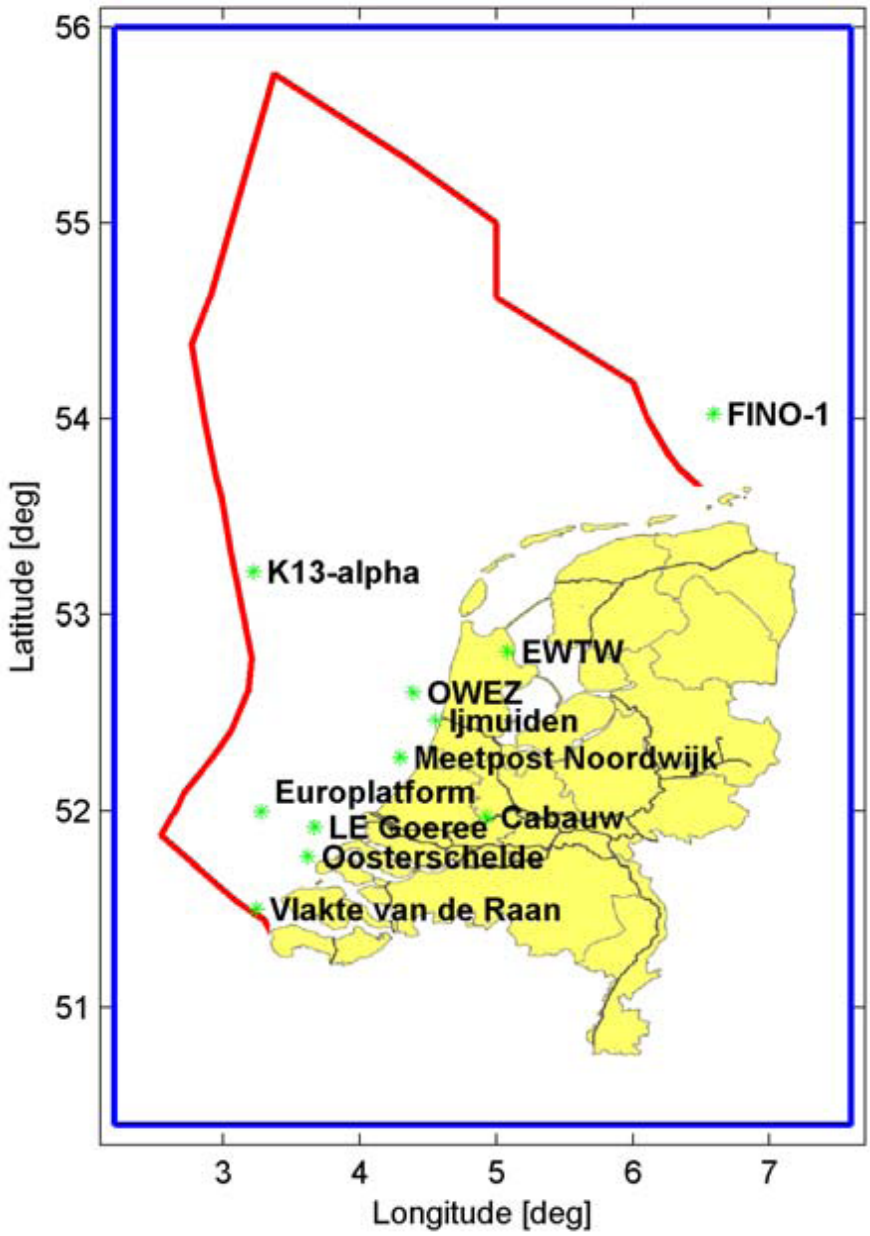

Figure 2.3 Measurements to validate the OWA-NEEZ wind atlas. Two onshore wind masts (Cabauw and EWTW, a wind mast at the ECN wind turbine test site Wieringermeer) and nine offshore locations were used (two offshore wind masts OWEZ and FINO1 and 7 off shore meteo-sites: Europlatform, K13, Meetpost Noordwijk, Ijmuiden, Lichteiland Goeree, Vlakte van de Raan and Oosterschelde). (source: Donkers, 2011).

2.3 NORSEWInD satellite wind climatology

For the EU_NORSEWInD project (Northern Seas Wind Index Database, www.norsewind.eu) which lasted from August 2008 to July 2012, ocean surface wind observations were retrieved from space (satellite remote sensing) and subsequently processed and analysed in order to provide new offshore wind climatology for the Baltic, the Irish and the North Sea (Bay Hasager et al., 2012).

The climatology maps are based on remote sensing winds (ASAR, QuikSCAT, ASCAT coastal wind product and SSM/I data) in combination with model data (ECMWF and Weather Research and Forecasting model WRF) and verified with observations.

Satellite scatterometer winds (SeaWinds scatterometer winds from the QuikSCAT satellite and ASCAT winds) are operational after extensive calibration and validation using advanced methods and are moreover routinely monitored for quality assurance[18]. Vogelzang et al. (2011) compared Buoy and scatterometer wind speed measurements to ECMWF weather model wind speeds at the horizontal resolution of 4 sorts of scatterometer products. The resolutions are: 25 (ASCAT-12.5), 50 (ASCAT-25), 100 (SeaWinds-KNMI) and 100 km (SeaWinds-NOAA). Generally, the smaller the Triple Collocation[19] random Error Standard Deviation, the better the mean wind on the resolved scale, indicating that scatterometer winds are very accurate as compared to ECMWF winds (version Januari 2009 which corresponds to ECMWF IFS cycle 35r3 with 25 km horizontal resolution) or the buoys in the climate-quality observation network (buoy winds are obviously more accurate on the local (point) scale). SAR winds (ASAR) have not been validated to the same extent. The accuracy of SSMI speeds has been found similar to those of SeaWinds.

Table 5. Triple Collocation Error Standard Deviations With Respect to the (Different) Scales Resolved by the Different Scatterometer Wind Products

	Buoy		ECMWF		Scatterometer	
Data Set	ε_u (ms^{-1})	ε_v (ms^{-1})	ε_u (ms^{-1})	ε_v (ms^{-1})	ε_u (ms^{-1})	ε_v (ms^{-1})
ASCAT-12.5	1.21	1.23	1.54	1.55	0.69	0.82
ASCAT-25	1.24	1.30	1.42	1.45	0.65	0.74
SeaWinds-KNMI	1.40	1.44	1.19	1.27	0.79	0.63
SeaWinds-NOAA	1.39	1.41	1.20	1.30	1.20	1.04

Table 2.1: Estimated global error budgets for diverse scatterometer products in the east-west (u) and north-south (v) wind components based on triple collocation for January 2009. Buoy winds are 10-minute mean winds from buoys positioned around the globe to monitor the climate (source: Vogelzang, 2011). The SeaWinds-NOAA[20] (QuikSCAT) and ASCAT-12.5 winds are used to make the NORSEWInD satellite wind climatology maps presented in sections 2.3.2. and 2.3.3.

[18] www.knmi.nl/scatterometer/ascat_osi_co_prod/ascat_app.cgi and http://research.metoffice.gov.uk/research/interproj/nwpsaf/scatter_report/nwp.html

[19] Triple collocation is a method of characterising systematic biases and random errors in in-situ measurements, satellite observations and model fields. It attempts to segregate the measurement uncertainties, geophysical, spatial and temporal representation and sampling differences in the different data sets by an objective method (Stoffelen, 1998; Vogelzang, 2011).

[20] SeaWinds-KNMI is based on a KNMI wind processor, which gives better results than the SeaWinds-NOAA processor: http://coaps.fsu.edu/scatterometry/meeting/docs/2013/First%20Results/Ebuchi_IOVWST2013.pdf:

When making a wind atlas from satellite observations, sampling biases have to be accounted for. Satellite observations are only made a few times a day and do not represent the average of the full diurnal cycle (the sampling bias is typically a few tenths of 1 m/s Ricardulli, 2013). Sampling errors can be corrected for by collocation procedures and need to be applied for all observation wind climatologies, but has generally not been performed. The same goes for biases caused by quality control (QC) procedures. An example of significant QC biases is found near the main harbours such as Rotterdam where large numbers of ships (about 100) are often waiting at the anchor areas and disturb the back scattered radar signal. QC screens some of the ship-reflection contaminated observations at low winds, but less so at high wind speeds (reduced contrast). The reduced sampling of low winds (compared to high winds) causes unrealistically high winds at anchor areas along the Dutch and Belgian coast.

Due to lack of resources, sampling and QC biases have not been accounted for in any of the NORSEWInD satellite wind products (ASAR, QuikSCAT or ASCAT).

2.3.1 Envisat ASAR

Climatology maps were made based on Synthetic Aperture Radar (SAR) images from the European Space Agency (ESA) satellite Envisat (2002 to early 2012). Most information is retrieved in 2010, fairly evenly distributed over the different months of the year and evenly distributed over the time when the satellite passes the area (local time: 21:30-22:00 northbound and 10:30-11:00 southbound). Figure 2.4 gives an indication of the spatial distribution of the number of SAR observations: the more overlapping “scenes”, the less uncertainly in the resulting wind map.

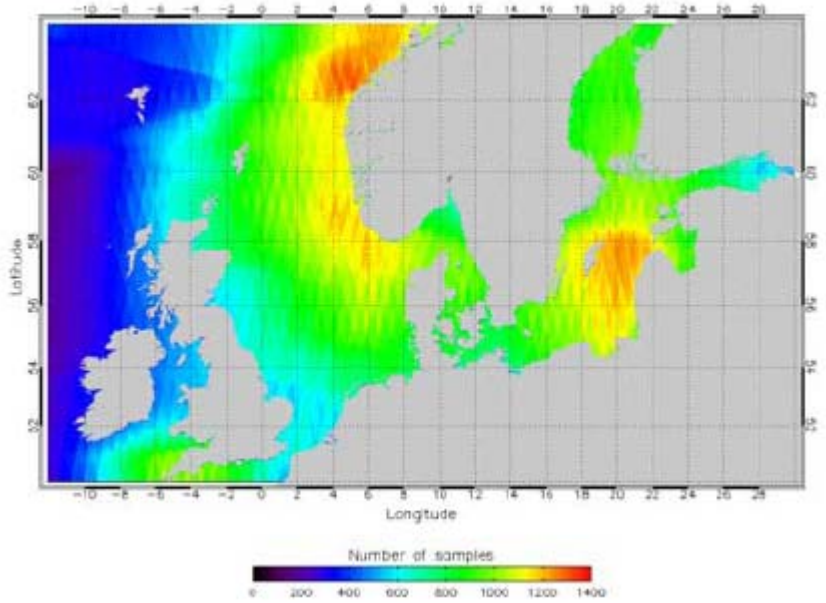

Figure 2.4: The number of overlapping Envisat ASAR scenes in wide swath mode (WSM) collected for the NORSEWInD project (Source: Hasager, 2012)

In order to get a homogeneous data set, all data are re-processed with CMOD5N and ECMWF wind direction as input (CMOD5N is a geophysical model function (GMF) for the transformation of C-band scatterometer data into 10 m equivalent-neutral wind speeds[21]; www.knmi.nl/scatterometer/cmod5). Finally, the resulting wind fields were used in S-WAsP (short for Satellite WAsP) software to calculate maps on a 2 km resolution of mean wind speed, Weibull scale and shape parameters and energy density (which depends on wind speed and air density), all at a height of 10 m (figure 2.5). Uncertainty estimates were made for all 4 parameters based on the number of satellite data used (fig. 2.4). This means that the uncertainty in the Weibull shape parameter and the energy density are larger than in the mean wind speed and Weibull scale parameter because for the Weibull shape parameter and the energy density more samples are necessary to get the same uncertainty.

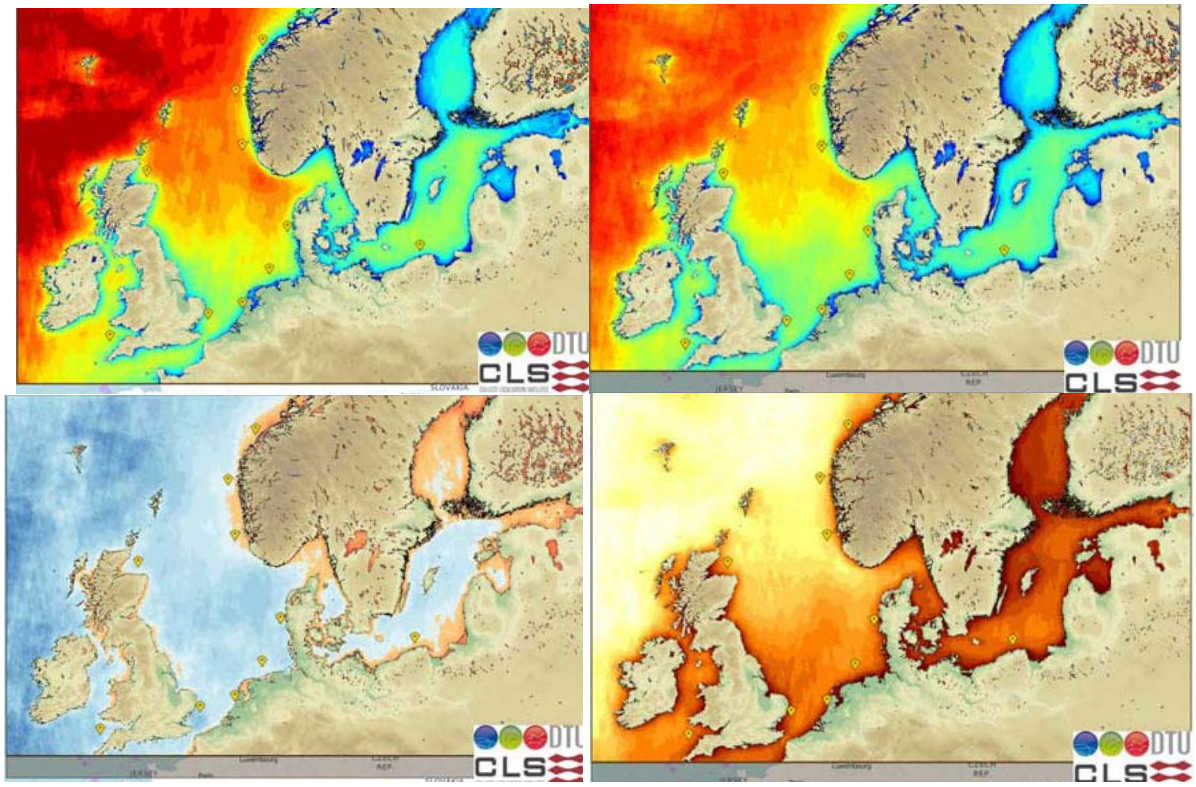

Figure 2.5 Envisat ASAR (2002-2012, with most data from 2010) mean wind speed (top left), Weibull scale parameter, which is a measure of the mean wind speed (top right), Weibull shape parameter (bottom left) and energy density (bottom right) all at 10 m height (source: Hasager 2012)

The SAR-based wind maps were compared to data from wind masts. SAR-winds are valid at 10m. In order to make a comparison possible, wind observations at heights other than 10 m were extrapolated to 10 m. For the North Sea five wind masts were used (Egmond aan Zee, Horns Rev M2, Fino-1, Horns Rev M7, Greater Gabbard) and where possible (for Egmond aan Zee and Horns Rev M2) a stability correction was performed. Also three different geophysical model functions (GMF's) were tested for Egmond aan Zee and Horns Rev M2, but for SAR wind speeds between 2-20 m/s the results were fairly comparable (not shown).

[21] A 10 m equivalent neutral wind speed is the wind speed at 10m height derived from the scatterometer roughness measurements at the sea surface assuming neutral stability and a logarithmic wind profile.

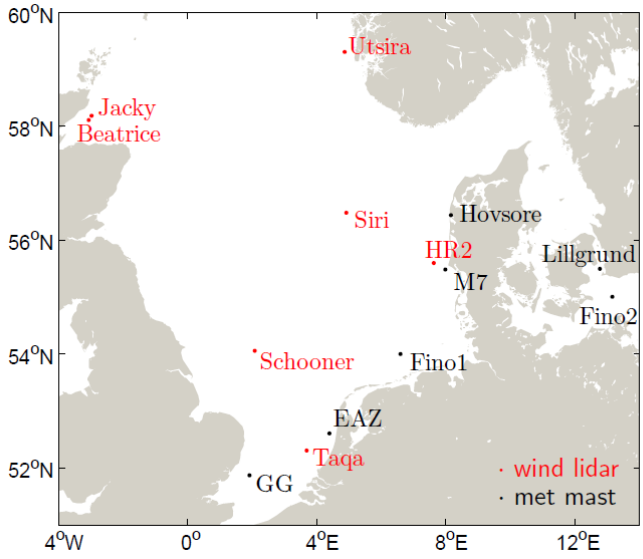

Table 1: NORSEWInD nodes information. Also displayed are the heigths of measurement of wind speed (WS), temperature (T), pressure (P), relative humidity (RH), wind direction (WD) and sonic (S)

Node	Node type	Period in DB	No. of 10 min	Height of WS AMSL [m]	Height of other measures AMSL [m]
Jacky	wind lidar WindCube	2010-11-10– 2011-11-09	923 5347	60–320 [60, 80, 100]	-
Siri	wind lidar WindCube	2010-06-02– 2011-05-02	6277 20243	85–345 [85, 105, 125]	-
Schooner	wind lidar WindCube	2010-07-16– 2011-11-09	24525 28572	76–216 [76, 92, 99]	-
Taqa	wind lidar WindCube	2010-02-25– 2011-03-19	38748 47317	70–250 [70, 90, 110]	-
HR2 (Horns Rev II)	wind lidar WindCube	2009-06-25– 2011-08-17	70650 94848	66–286 [66, 86, 106]	-
Utsira	wind lidar WindCube	2009-09-28– 2011-07-01	33649 59908	67–300 [67, 80, 100]	-
Beatrice	wind lidar ZephIR	2010-11-10– 2011-02-25	9034	[52.5, 75.5, 90.5... 105.5, 162.5]	-
Høvsøre (flat and homo.)	met mast	2004-02-28– 2011-12-18	60828	[10, 40, 60... 80, 100]	S-10
M7 (Horns Rev I)	met mast	2005-01-01– 2009-12-15	297826	[20, 30, 40... 50, 60, 70]	P-16 WD-[28, 68] T-[-3, 16, 64]
Fino 1	met mast	2003-07-30– 2010-05-01	28530 85942	[33, 40, 50, 80, 90, 100]	T-[-3, 30, 40, 50, 70, 100] P-[20, 90] WD-[33, 40, 50, 60, 80] RH-[33, 50, 90]
Lillgrund	met mast	2009-01-01– 2009-12-31	52482	[13, 20, 40... 63, 65]	P-5, RH-7 T-7, WD-[18, 61]
Fino 2	met mast	2007-07-31– 2010-04-30	66991 75244	[32, 42, 52, 62... 72, 82, 92, 102]	WD-[31, 51, 71, 91] RH-[30, 50, 99] T-[30, 40, 50, 70, 99] P-[30, 90]
EAZ (Egmond aan Zee)	met mast	2005-07-01– 2008-12-31	4501 96185	[21, 70, 116]	RH-[21, 70, 116] P-20, WD-[21, 70, 116] T-[-3.8, 21, 70, 116]
GG (Greater Gabbard)	met mast	2006-01-23– 2010-07-12	222033	[42.5, 52.5, 72.5... 82.5, 86.5]	WD-62.5, P-84.5 T-84.5, RH-38.5

Figure 2.6 on the top panel the NORSEWInD network of meteorological and LIDAR stations in North Sea and Baltic Sea (e.g. HR2 = Hors Rev M2, M7 = Horns Rev M7, GG = Greater Gabbard, EAZ = Egmond aan Zee) and on the panel below information on measurements (source: Peña, 2012)

Lifting winds to 100 m in NORSEWInD

step 1: estimate u_{*SAR} (friction velocity based on the 10m SAR-wind) through iteration assuming a logarithmic wind profile (2.1a) and a roughness length according to Charnock (2.1b):

$$u_{10SAR} = u_{*SAR} / \kappa \, [\ln (10/z_0)] \qquad (2.1a)$$

$$z_0 = \alpha_c (u_*^2 / g) \qquad (2.1b)$$

- u_* = friction velocity
- κ = von Kármán constant (0.04)
- z_0 = surface roughness
- α_c = Charnock constant (0.01445)
- g = acceleration of gravity (9.8 m/s^2)

step 2: estimate Obukhov length $L_{WRF/SAR}$ from u_{*SAR} (based on SAR wind) and WRF parameters $T2_{WRF}$ and HFX_{WRF} (2m absolute temperature and surface heat flux):

$$L_{WRF/SAR} = - (T2_{WRF} \, u_{*SAR}^3) / (\kappa \, g \, HFX_{WRF}) \qquad (2.1c)$$

Formulas 2.1c and 1.3b are equal as $C_p \approx 1$ (C_p Air (Sea level, dry,0 °C (273.15 K)) = 1.0035 and C_p Air (typical room conditions) = 1.0122 J/(gK)

step 3a: for unstable conditions ($L_{WRF/SAR} \leq 0$) calculate wind at 100 m using the Businger-Dyer formula (2.1d)

$$u(z) = u_{*SAR}/\kappa \, [\ln(100/z_o) - \psi(100/ L_{WRF/SAR})] \quad \text{(Businger-Dyer formula)} \qquad (2.1d)$$

step 3a: for stable conditions ($L_{WRF/SAR} > 0$) calculate wind at 100 m using an adapted Businger-Dyer formula (2.1e)

$$u(z) = u_{*SAR}/\kappa \, [\ln(100/z_o) - \psi(100/ L_{WRF/SAR}) * (1-100/2PBLH)] \qquad (2.1e)$$

- PBLH = Planetary boundary layer height from WRF
- Stability function ψ_m according to formula 1.12 (with L = $L_{WRF/SAR}$ from formula 2.1c):

$$\psi_m = 3/2 \ln [(1 + x + x^2) / 3] - \sqrt{3} \arctan [(2x+1) / \sqrt{3}] + \pi / \sqrt{3}$$

$$\text{where } x = [1 - 12 (z / L)]^{1/3} \quad \text{(unstable conditions } z/L \leq 0) \qquad (1.12a)$$

$$\Psi_m (z/L) = -4.7 \, z/L \quad \text{(stable conditions } z/L > 0) \qquad (1.12b)$$

First attempts have been made to lift the satellite wind products at 10m to hub height (in this case 100m). This is done by combining satellite wind speed information at 10 m with temperature and heat flux (which determine stability) from a numerical weather forecasting model, in this case Weather Research and Forecasting model WRF. The satellite SAR wind

speeds are lifted to 100 m with a Businger-Dyer formula which is adapted for stable conditions so that it depends on the height of the planetary boundary layer (PBL of WRF is used). The Monin-Obukhov length is determined with SAR-based wind speeds and with air temperature and heat flux from WRF. A simple Charnock relation with a Charnock constant of 0.01445 is used to model the roughness at sea (see discussion in section 1.1.3). For stable conditions, stability function Ψ (z/L) is equal to the one used in the European Wind Atlas (formula 1.12b = 1.6b). For unstable conditions it is different (1.12a). The formulas used are given in the blue panel above.

For the period from 1 May 2006 to 1 May 2007 (with 80 Envisat ASAR scenes) a comparison was made between the lifted SAR-wind speeds and the WRF simulations at 100 m. It appeared that lifted SAR-winds were consistently lower than the WRF simulations with the largest difference near the Dutch and German coast (figure 2.7). Research mast FINO-1 is in this area and a comparison with FINO-1 data showed that both the lifted SAR-winds and the WRF-simulations underestimated the wind speed at 100 m (not shown) and that the lifted SAR-winds show the highest spread (not shown).

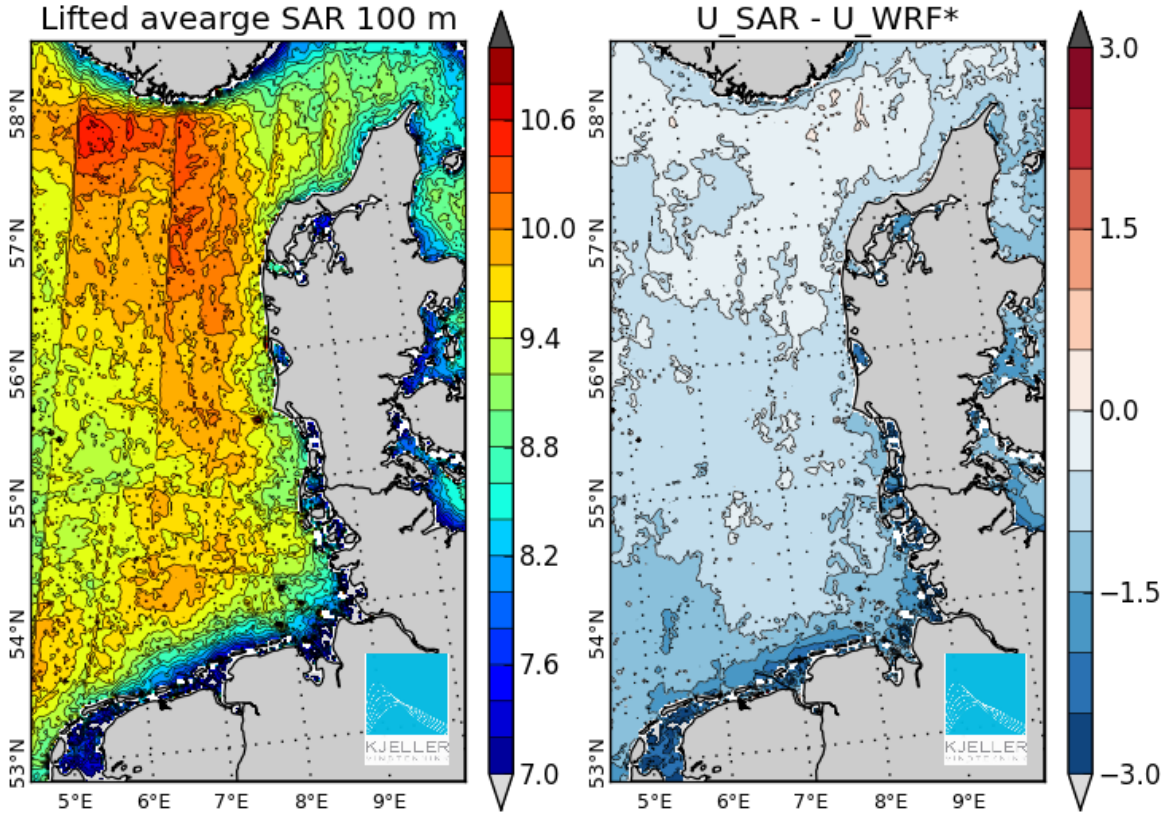

Figure 2.7 Mean wind speed (m/s) from a total of 80 SAR scenes lifted to 100 m using stability and PBL height information from WRF (left panel) and a plot of the difference between 100-m SAR and WRF wind speeds (m/s) where U_WRF indicates WRF simulations concurrent with the SAR data acquisitions (right panel). (Source: Hasager, 2012).*

The main limitations for using SAR winds at 100m are:

- A SAR measures ocean roughness and the change of wind with height needs to be modelled with ancillary information (e.g. SST and free-troposphere wind)
- SAR systems are not well calibrated (accuracy/precision: ~0.5 m/s)
- SAR data need to be reprocessed with wind directions from a Numerical Weather Prediction (NWP) model (in this case ECMWF) to get a homogeneous data set, but all NWP models are known to be systematically biased in stable conditions (see section 3.3). For the ASCAT and SeaWinds products (2.3.2 and 2.3.3) no NWP wind direction is required: the wind direction is directly measured by the scatterometer.
- QC is applied and sampling bias needs to be accounted for. This is the same for the ASCAT and SeaWinds products (2.3.2 and 2.3.3).

Within the NORSEWInD project wind mast and Lidar wind measurements have been used to improve knowledge of the vertical profiles of wind speed and vertical wind shear (the rate of change of wind speed with height) (Peña 2012). This knowledge is important for (among other things): predicting winds at heights other than measurement height; predicting wind turbine power production (this is normally predicted using only the hub-height wind speed but the average speed over the whole height of the rotor gives better predictions); predicting design loads and wake effects. In order to study the vertical wind shear dependency on atmospheric stability (including the factors fetch, mean wind speed, seasonality), a multi-variational correlation analysis was performed with the vertical wind shear observed at a height of about 100m in the NORSEWInD network (meteorological wind masts and LIDARs). Wind data from the WRF numerical weather forecasting model are evaluated and used to construct a means of determining the long-term vertical profiles of wind speed and wind shear. A method developed to extrapolate satellite surface winds to 100 m based on these measured and modelled winds is incorporated in the NORSEWInD wind maps. Peña (2012) found that the influence of both stability and the height of the planetary boundary layer (PBL) should be taken into account when extrapolating winds to higher levels, but unfortunately WRF's representation of the PBL height and sea surface temperature (which influences stability) is rather poor (Ad Stoffelen KNMI).

Some of Peña's (2012) major findings are:

- **Wind lidars** provide valuable information of the vertical wind shear within a wide geographical area and range of vertical levels in the atmosphere that is nearly impossible to obtain with the current met mast network in the North Sea. There are also no mast and boom distortion related effects when a wind lidar is used.
- The commonly adopted **offshore vertical wind shear value**, $\alpha = 0.2$, is valid for a very narrow set of atmospheric and marine conditions: α varies in the marine Surface Boundary Layer with **atmospheric stability, roughness** (sea roughness increases with wind speed) and height. Above the surface layer, other effects, such as the **Boundary Layer Height and baroclinicity**, become more important. For the same height and roughness, α is higher during stable than unstable conditions.
- **Offshore the observed α values at 100 m height are often within the range -0.2-0.8 with a peak within the range 0-0.125**. Negative values are found both under unstable and stable atmospheric conditions. The centroid of the distribution of these α values is generally found to be close to that value estimated from the neutral log wind profile assuming neutral conditions and $z_o = 0.0002$ m. In onshore conditions α increases, mainly due to the higher roughness length.
- α is found to be nearly constant during the **diurnal cycle**, because of the slight diurnal variation of the sea temperature (as opposed to the situation onshore). On a **monthly basis**, α is generally found to be highest and lowest during the spring and autumn months, respectively. This is due to the seasonality of the sea temperature, which during spring is still cold from the winter, while the air is warming up, thus giving rise to stable conditions; during autumn the sea is still warm, while the air starts to cool down, thus giving rise to unstable conditions.
- No clear indication of α **dependency on distance to the coast** is found. Most of the NORSEWInD nodes exhibit an **increasing α for increasing wind speeds**, since the sea roughness increases with wind speed. Furthermore, for most nodes the behavior of α with wind speed is well predicted by using the neutral wind speed profile and Charnock's relation within the range 5-10 m/s and under-predicted for higher wind speeds. When analyzing the **seasonality of α**, it is generally found that the predicted α values assuming neutral conditions are below the observed values, indicating a general stable correction to the vertical wind shear over the North Sea. Classifying observations of α into unstable and stable atmospheric conditions (based on observed stability measures), we clearly find a higher α value for stable than for unstable conditions, as expected.
- When extrapolating winds using profile formulations that take into account the **influence of both stability (from WRF or observations) and** the **Boundary Layer Height**, we find the highest correlations compared to the observations, only in the cases where the stability measures are accurate and the low-level measurement is not distorted. By using stability information only, we find the lowest correlations.

2.3.2 QuikSCAT SeaWinds

Climatology maps were also made based on images from the SeaWinds scatterometer (QSCAT) from the National Aeronautics and Space Administration (NASA) satellite QuikSCAT. This satellite provided twice daily near global coverage of data for more than 10 years (July 1999-November 2009). For the NORSEWInD project all rain-flagged data were excluded from the analysis (rain-contaminated wind speeds are biased towards higher wind speeds). This leaves about 7000 rain-free wind retrievals for all North Sea locations (figure 2.8).

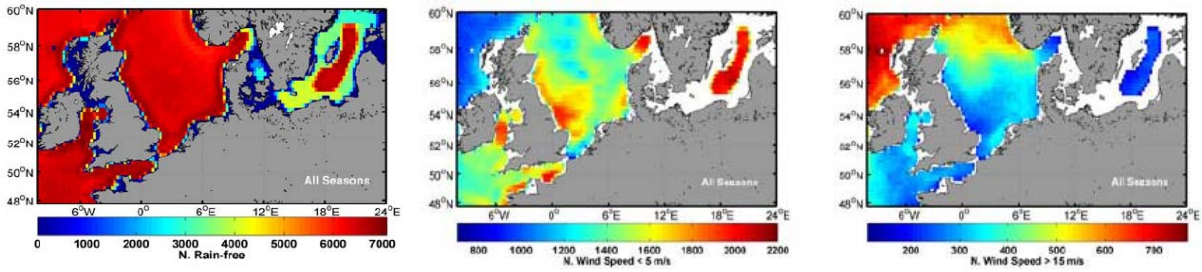

Figure 2.8 Number of rain-free QuikSCAT wind retrievals from August 1999 to October 2009 (left) with wind speed lower than 5 m/s (middle) and higher than 15 m/s (right) (source: Hasager, 2012).

Uncertainty estimates for mean wind speed, Weibull shape and scale parameter and energy density are based on the number of satellite data used (figure 2.9).

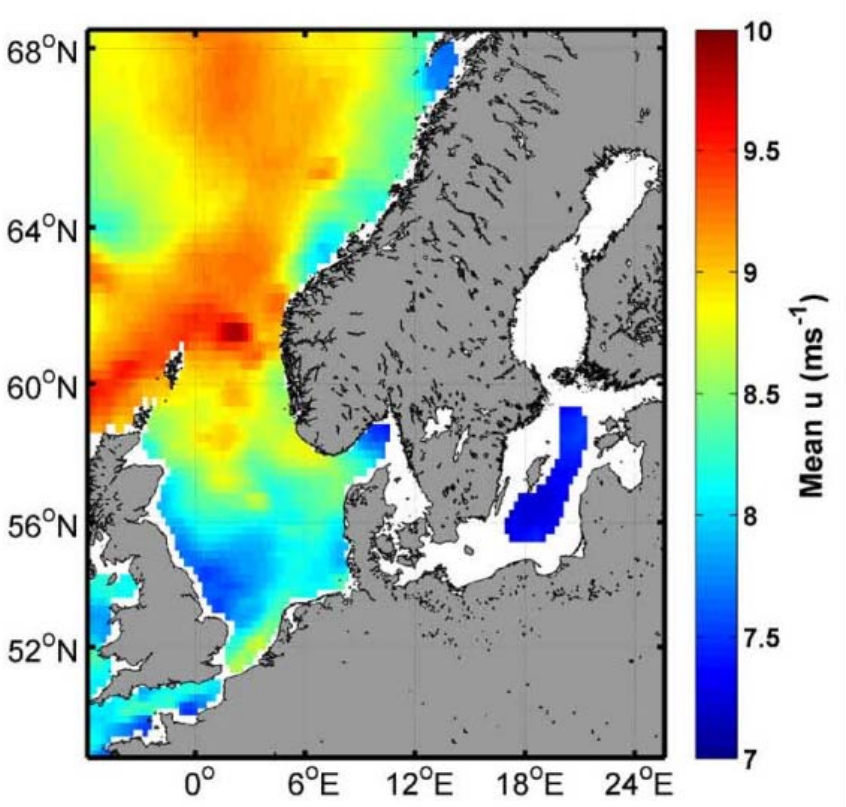

Figure 2.9 QuikSCAT wind atlas (1999-2009) (source: poster Living Planet Symposium Edinburgh (2013): http://orbit.dtu.dk/ws/files/59448583/Wind_atlas_of_the_Northern_European_Seas.pdf

The QuikSCAT wind atlas (fig, 2.9) has a lower spatial resolution than the Envisat ASAR map (par 2.3.1), but the advantage is that it gives a better description of the long term behaviour of the wind. QuikSCAT stopped operation at the end of 2009, but other scatterometers such as ASCAT are still operating and it should be possible to merge the data to produce a dataset covering a longer period.

All QuikSCAT winds are validated against 10m equivalent neutral wind speeds[22] from buoy measurements. Sousa et al (2013) have shown that for the Galician coast wind speeds from QuikSCAT and WRF (nov 2008-oct 2009; resolution 4 km) are similar. Quikscat winds are accurate in open sea up to 25 km from the coast. Comparing the two datasets to the buoy 10 m wind speeds reveals RMS errors of 1.3 m/s (QuikSCAT) and 1.9 m/s (WRF) for the wind speed range important for wind energy production (3.4-10.7 m/s). The QuikSCAT bias was 0.3 m/s and the WRF bias was less uniform, being 0.1, -0.1 and -0.5 m/s compared to the three buoys (30-48 km offshore). In Karagali et al (2012) QuikSCAT ocean wind speed and direction were compared to observations from three offshore wind masts: HornsRev (M2), Fino-1 and Greater Gabbard (locations are shown in figure 2.6). Mean biases (in-situ minus satellite) are close to zero for wind speed and -2.7° for wind direction with a standard deviation of 1.2 m/s and 15° respectively. Comparison of QuikSCAT and WRF-climatology is summarised in figure 2.10.

[22] A 10 m equivalent neutral wind speed is the wind speed at 10m height derived from the buoy winds at the sea surface assuming neutral stability and a logarithmic wind profile.

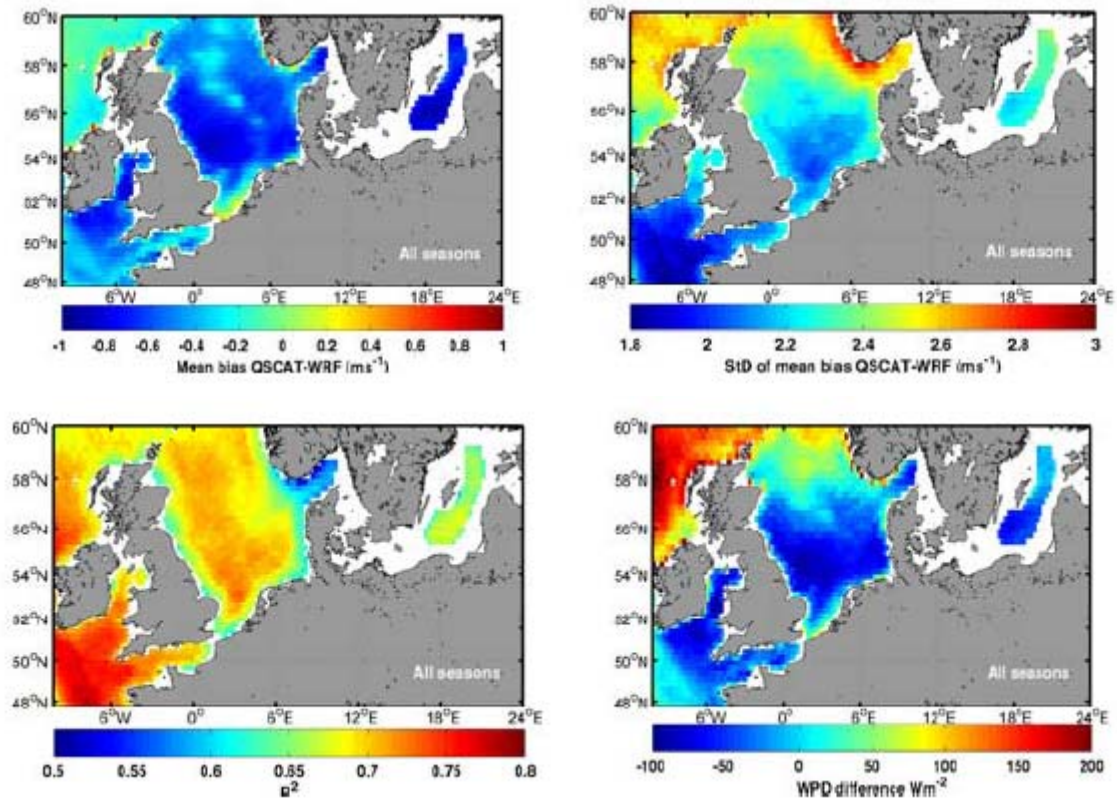

Figure 2.10 Comparison QuikSCAT and WRF: for most domains WRF gives higher wind speeds than QuikSCAT (bias mean wind speed QuikSCAT – WRF is negative), except offshore from the Netherlands where the bias is positive (top left panel). The standard deviation of the mean bias increases towards the north and is highest in the North Atlantic and near the Norwegian coast (top right panel). Correlation coefficient R^2 (bottom right panel) is lower in coastal areas than further offshore because of increased wind variability near the coast (bottom left panel). Wind Power Density (WPD) is proportional to wind speed^3. On the central North Sea WPD difference (QuikSCAT – WRF) is negative and WPD based on WRF is up to 100 W/m^2 higher than the one based on QuikSCAT. Note the light blue spots in the North sea bias of WRF minus QSCAT. These are due to the oil platforms and ships that contribute radar backscatter by corner reflections. At low winds these are noted and removed by Quality Control procedures; this enhances the mean QuikScat winds. Errors due to QC still need to be removed from the satellite wind maps as do sampling errors (source: Hasager, 2012).

2.3.3 ASCAT coastal L3 wind product

Since November 2009 KNMI produces the coastal ASCAT (Advanced Scatterometer) product on behalf of EUMETSAT. This product consists of measurements of wind speed and direction (equivalent neutral at 10 m[23]) within a wind vector cell of size 12.5 km. For the period 1 June 2007 to 31 December 2008 the full resolution product of ASCAT was reprocessed and gridded into the ASCAT coastal L3 product for the North Sea and the Irish Sea (also on a 12.5 km grid). The ASCAT satellite passes the North Sea twice a day: south bound around 09:00 AM UTC and north bound around 22:00 PM UTC.

Uncertainty estimates are made only for mean wind speed and are based on the number of valid grid points used for the calculation of the averaged wind speed map (figure 2.11).

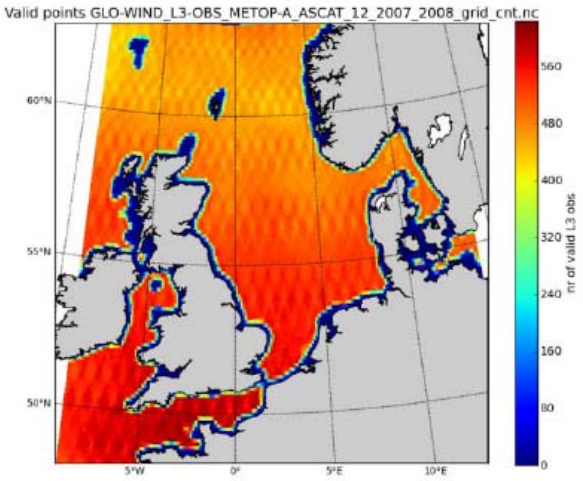

Figure 2.11 Total number of valid grid points used for the calculation of the averaged wind speed map

The ASCAT coastal L3 product[24] is calibrated, validated and routinely monitored against buoys. It is also compared in near real time to ECMWF model winds for quality assurance.

As mentioned at the beginning of this chapter, QC biases cause unrealistically high winds along the Dutch and Belgian coast (figure 2.12). Note that the North Sea oil platform effects visible in QuikSCAT are smaller here. Contamination effects occur for QuikSCAT and SAR as well, but here not the same QC is applied.

The ASCAT coastal L3 product has also been compared to WRF. Comparison between ASCAT and WRF for the period between June 2007 and November 2008 is summarised in figure 2.13. The RMSD of ASCAT-WRF wind speeds are much higher than for ASCAT-ECMWF and the correlation coefficients lower, indicating that WRF wind speeds are less accurate than ECMWF wind speeds (not shown).

[23] A 10 m equivalent neutral wind speed is the wind speed at 10m height derived from the scatterometer roughness measurements at the sea surface assuming neutral stability and a logarithmic wind profile.
[24] Full name: EU Copernicus MyOcean Marine Core Services ASCAT coastal L3 product

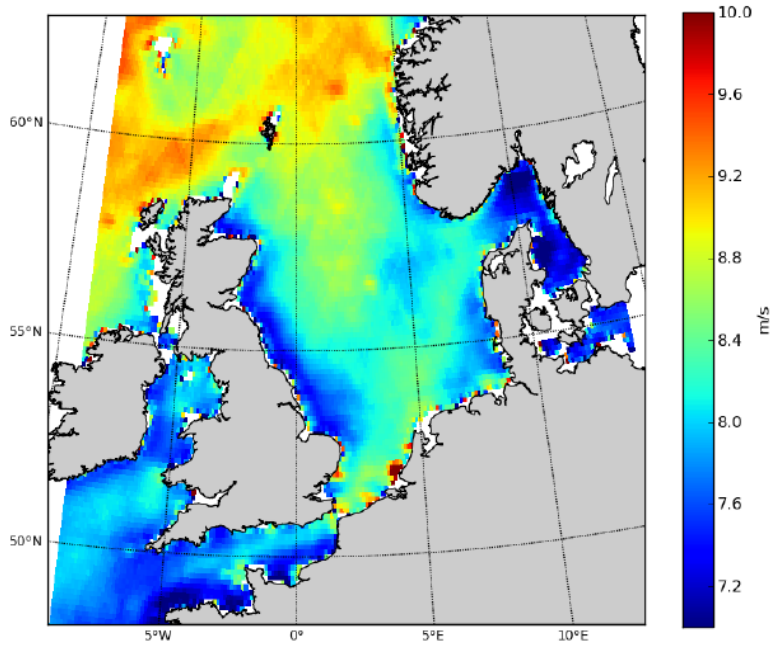

Figure 2.12 ASCAT coastal wind atlas (2007-2008) from KNMI OSI-SAF (source: poster Living Planet Symposium Edinburgh (2013): http://orbit.dtu.dk/ws/files/59448583/Wind_atlas_of_the_Northern_European_Seas.pdf)

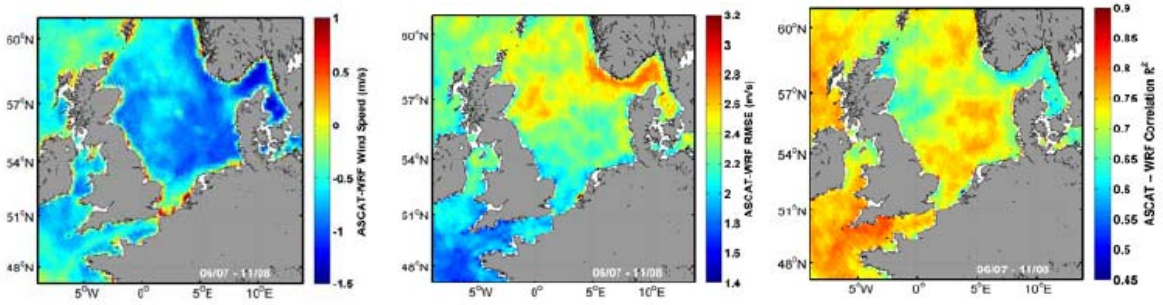

Figure 2.13 Comparison ASCAT and WRF: for most domains WRF gives higher wind speeds than ASCAT (bias mean wind speed ASCAT – WRF is negative), except offshore from the Netherlands where the bias is positive (left panel). The Root Mean Square Difference (RMSD) generally increases towards the north, but is very high for the Rotterdam area, more than 3 m/s (middle panel). The correlation coefficient R^2 (right panel) is lower in coastal areas than further offshore (source: Hasager, 2012).

A triple collocation method[25] is routinely applied on a set of the ASCAT coastal winds, in-situ winds and ECMWF winds. Climatological spatial representation errors are taken into account when comparing these wind speeds as scatterometer, buoy and ECMWF winds have different spatial representations and consequently different climatological distributions. Data from the Egmond aan Zee meteorological mast, ASCAT and model data from the WRF climatology run for June 2007 until November 2008 have also been used in triple collocation, but this needs further evaluation, since the results appear different from the multi-year observation station statistics performed over the globe.

[25] Triple collocation is a method enabling to characterise systematic biases and random errors in in-situ measurements, satellite observations and model fields. It attempts to segregate the measurement uncertainties, geophysical, spatial and temporal representation and sampling differences in the different data sets by an objective method (Stoffelen, 1998; Vogelzang et al., 2011).

2.3.4 SSM/I

The satellite images from the Spatial Sensor Microwave Imager (SSM/I) of the Defence Meteorological Satellite Program (DMSP) cover the longest period, from September 1987 onward, which makes these data very valuable for sampling the long term variability of the wind climate. The limitations of SSM/I are that it is wind speed only and that coastal and rain areas are not covered.

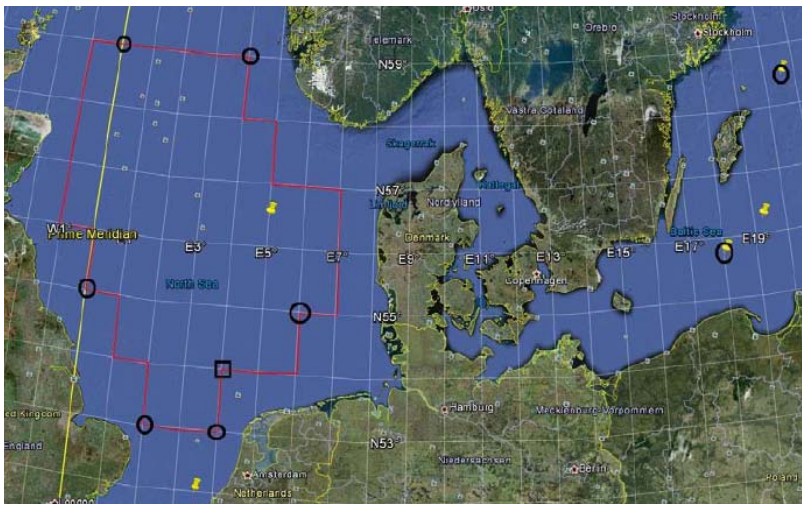

Figure 2.14: SSM/I data used for all points at full degrees longitude and latitude at and within the shown red border plus the five points at the yellow Google placemarks (needles). Black circle points indicate points where trends in wind power index have been calculated, for the black square point a monthly analyses has been done (source: Hasager, 2012).

In the NORSEWInD project a study was done to estimate trends in offshore wind power. Where possible two wind speed measurements per day were used for 24 years (1988-2011) for six of the fifty points in the North Sea and for two of the three in the Baltic Sea (figure 2.14). Wind speeds at 100 m were derived from these SSM/I data assuming a logarithmic wind profile (neutral stability) and the Charnock roughness formula for open sea ($\alpha = 0.011$ which is a bit lower than in WAsP and for the lifted SAR winds described in section 2.3.1 where the Charnock constant is assumed to be 0.014). Based on these 100-m wind speeds, wind power indices were calculated assuming that wind turbines operate for wind speeds between 5 and 25 m/s and that their power curves are approximately parabolic until 15 m/s and constant above. There is no significant correlation between the wind power index and the NAO-index[26] for any of the six North Sea points, but for all points the power index (which in this study is assumed to be dependent on the wind speed squared) increases while the NAO-index decreases. This is not what you would expect because the power index only depends on the wind speed in this study and the NAO-index shows that the wind speed decreases. Furthermore, it is common knowledge in the wind energy community that there has been a decrease wind energy yields since 1990 and that 2010 was a particularly bad year.

[26] NAO (North Atlantic Oscillation) Index is a measure for the difference in air pressure between Iceland and the Azores (used: http://www.cpc.ncep.noaa.gov/products/precip/CWlink/pna/norm.nao.monthly.b5001.current.asci)

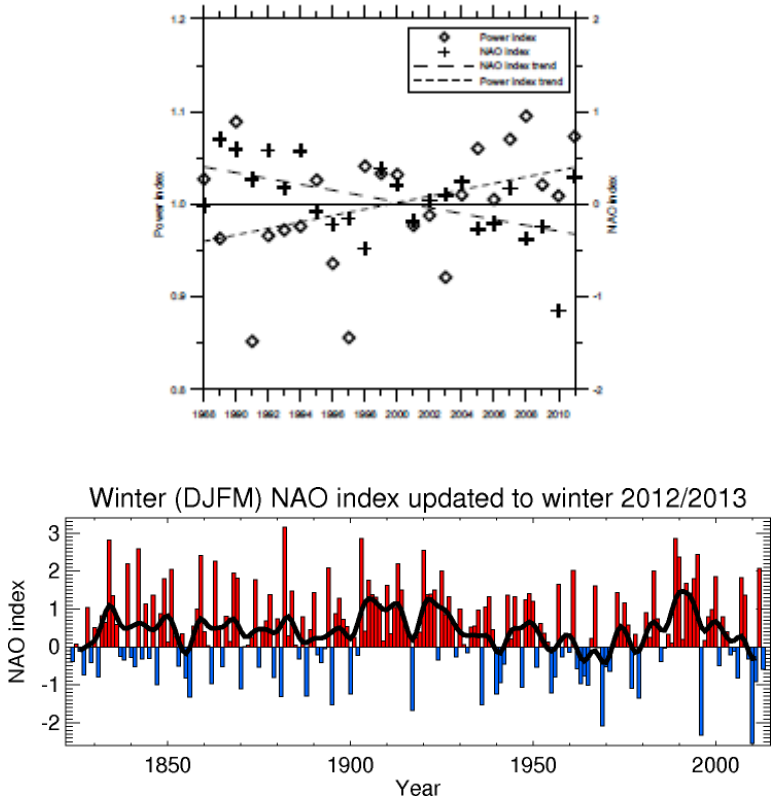

Figure 2.15 Upper panel: Trend in normalized power index at 53N, 2E compared to trend in NAO-index (source: Hasager 2012). Lower panel: winter NAO-index updated to the winter of 2012/13. Note the upward trend from the 1960s to the early 1990s, but also that the trend has not been sustained and has significant year-to-year variability superimposed on it. Note also that the winter 2009/10 had the most negative NAO index measured during the almost 190-year record.(source: http://www.cru.uea.ac.uk/~timo/datapages/naoi.htm).

3 Limitations of wind atlases and weather forecasting models

3.1 Long-term variability of the wind climate

For all wind atlases it is important to realise what period they are based on. By analysing long series of pressure readings in e.g. the Netherlands, Scotland and Denmark, Bakker (2011) found that, although there has been no significant long term trend in the geostrophic wind[27] above the North Sea in the past 130 years, there are 'windy' periods and 'calmer' periods (figure 3.1). This is what we refer to as the natural long-term variability of the current wind climate: the highest 11 year average is about 10% higher than lowest.

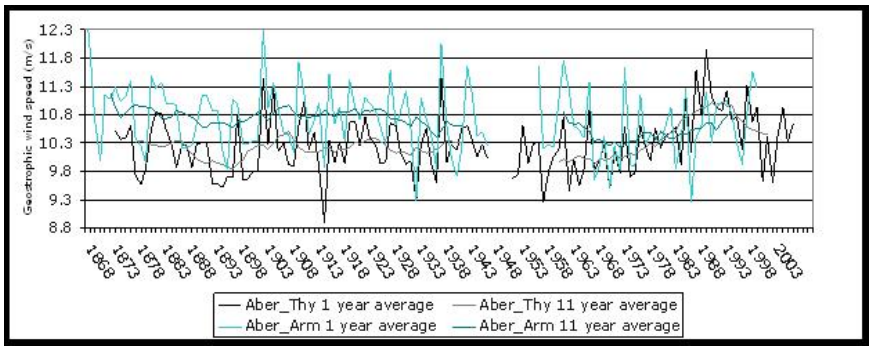

Figure 3.1 Geostrophic wind (1 year and 11 year average) calculated with pressure readings at Aberdeen_Amargh_De Bilt (1868-2000) and Aberdeen_Thyboron_De Bilt (1874-2007) (source: Bakker, 2011)[28].

The yearly averaged wind speed at Cabauw (1986-2011) shows the calmer period around 2010 compared to the windier period around 1990 (figure 3.2).

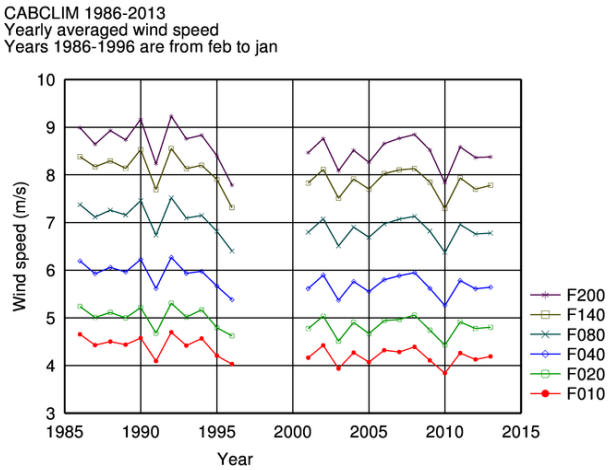

Figure 3.2 Yearly averaged wind speed Cabauw1986-2013 (1986-1996 are from February to January) (source: http://www.knmi.nl/~bosveld/)

[27] Geostrophic wind is a theoretical wind just above the planetary boundary layer (PBL) which is the result of the balancing of two forces: the pressure gradient and the Coriolis force (curved isobars and the centripetal force caused by this are not taken into account, nor the isallobaric effect which is the effect of pressure changes). The true wind also depends on the friction from the ground, but is assumed negligible above the PBL .

[28] KNMI has the intention to extend figure 3.1 to 2013. No data are available during the second world war.

The existing wind atlases do not include the long-term variability of the current wind climate (figure 3.3). Most of the existing atlases or maps are based on periods where the geostrophic wind was relatively low (e.g., the European Wind Atlas which is based on wind measurements from 1970-1976, the OWA-NEEZ map which is based on data from 2003-2009, the Envisat ASAR NORSEWInD maps based on satellite images from 2002-2012 with a focus on 2010 and the ASCAT NORSEWInD maps based on satellite images from 2007-2008). Only the KEMA/SenterNovem Wind Atlas (1983-2002) and SSM/I atlas (1988-2011) are based on measurements including in a relatively windy period, which in the case of KEMA/SenterNovem is too windy.

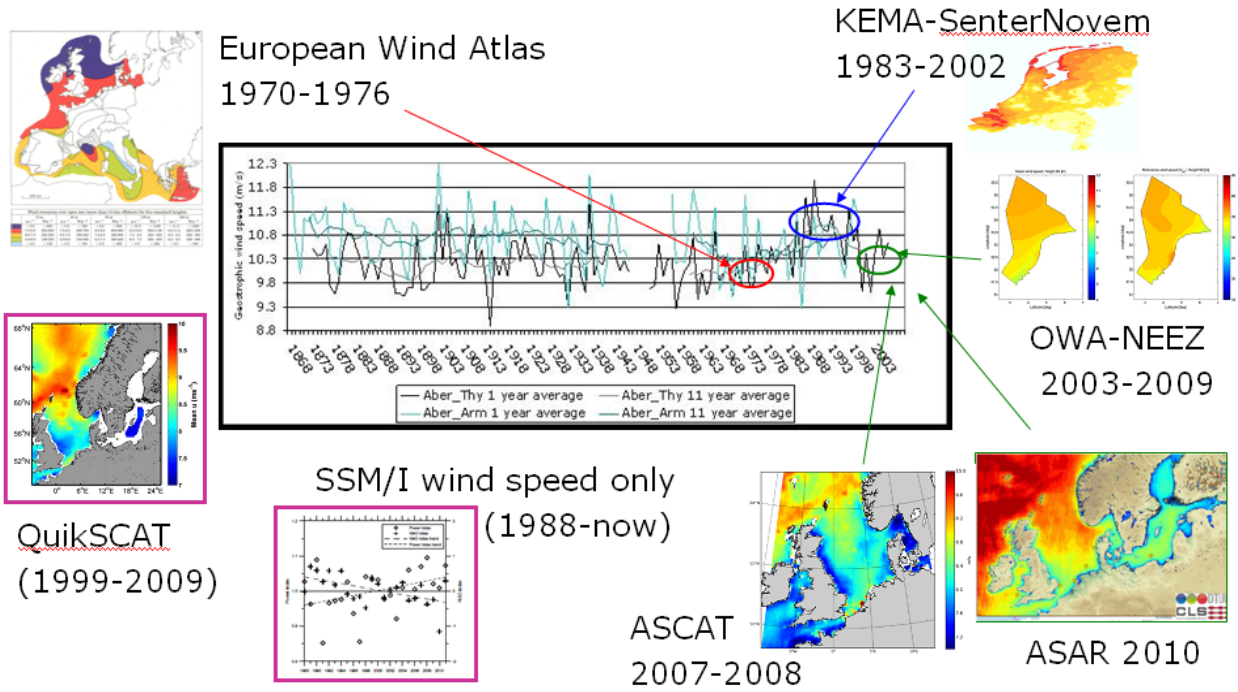

Figure 3.3 Existing wind atlases do not include the long term variability of the wind climate

The NORSEWInD QuikSCAT map is based on a 10 year period (1999-2009) that should cover most of the long-term wind climate variability, but QuikSCAT data are collected only twice a day and rain-contaminated data are excluded. These sampling errors can be corrected for by collocation procedures, but the NORSEWInD project lacked funding to do so.

SSM/I satellite data (1988-present) which are available six times a day cover the longest period which makes this data set the most promising one for quantifying the long-term variability of the wind climate. The results of the trend study based on SSM/I satellite data are however strange (Hasager, 2012). The wind power index (which in the definition used only depends on the wind speed squared) increases (although only slightly) with decreasing NAO-index.

Ricciardulli et al (2013) are doing work on integrating observations from multiple scatterometers into a climate data record (figure 3.4).

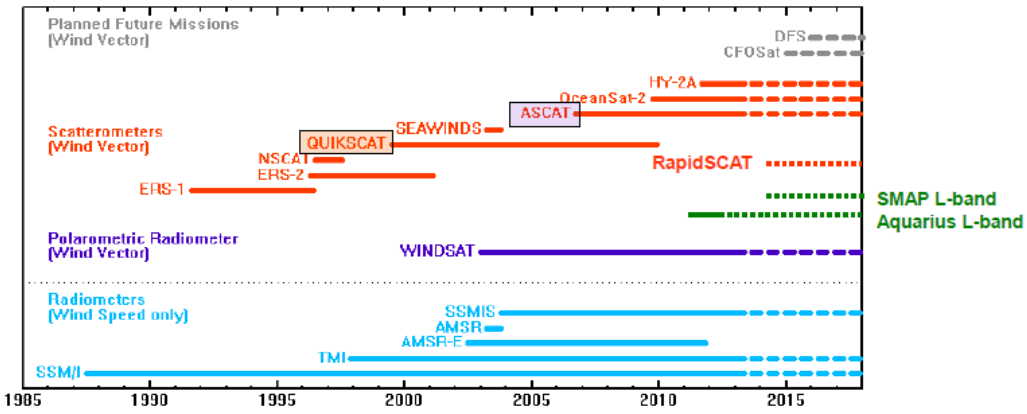

Figure 3.4 Overview of Ocean Vector Wind Missions: the idea is to start with ERS (windvector) in 1991 and with SSM/I (wind speed) in 1987 and to use ASCAT as a follow-up of QuikSCAT. RapidSCAT can be used to get a better understanding of the diurnal cycle (source: Riccardulli, 2013).

By using the 34-year ERA-Interim reanalysis the long-term variability of the current wind climate is included in the model wind climatology constructed by KNMI.

3.2 Resolution and vertical range

3.2.1 Horizontal resolution

Figure 3.5 illustrates the problems that arise when the horizontal resolution is course. Especially coastal areas are incorrectly modelled: this due to the large area of the model grid-box, but is made worse by a lack of detail in the model's coastline.

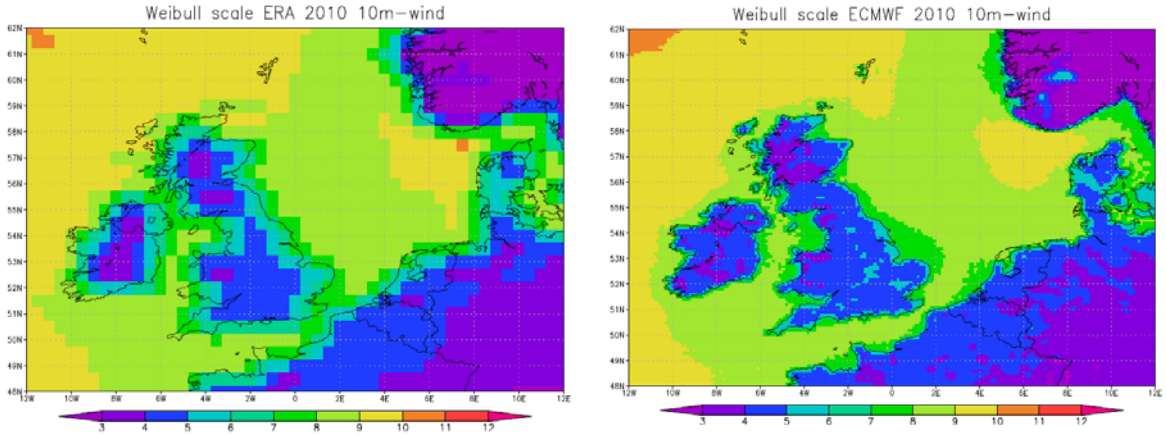

Figure 3.5 Weibull scale parameter for 2010 (at 10 m height) based on ERA-Interim on a 80 km grid (left panel) and the operational forecasting model ECMWF on a 16 km grid (right panel). Note that the patterns are largely similar on the North Sea, but differ in coastal areas.

In weather forecasting models diffusion operators are used to avoid numerical instability[29] which would cause the model to malfunction. However, there is a price to pay for numerical stability: the horizontal resolution of spectral models[30] effectively becomes 5-10 times courser.

A grid spacing of 80 km, such as in ERA-Interim, implies an effective horizontal resolution of 400-800 km (Shamarock, 2006). For the operational weather forecasting model ECMWF that was used in this study (grid spacing 16 km), the effective horizontal resolution is about 110 km (figure 3.6). Marseille et al (2013) found an even greater effect and concluded that the effective horizontal resolution of global models is 200-500 km above sea and in the upper air, i.e., substantially lower than the typical model grid size of 10-20 km.

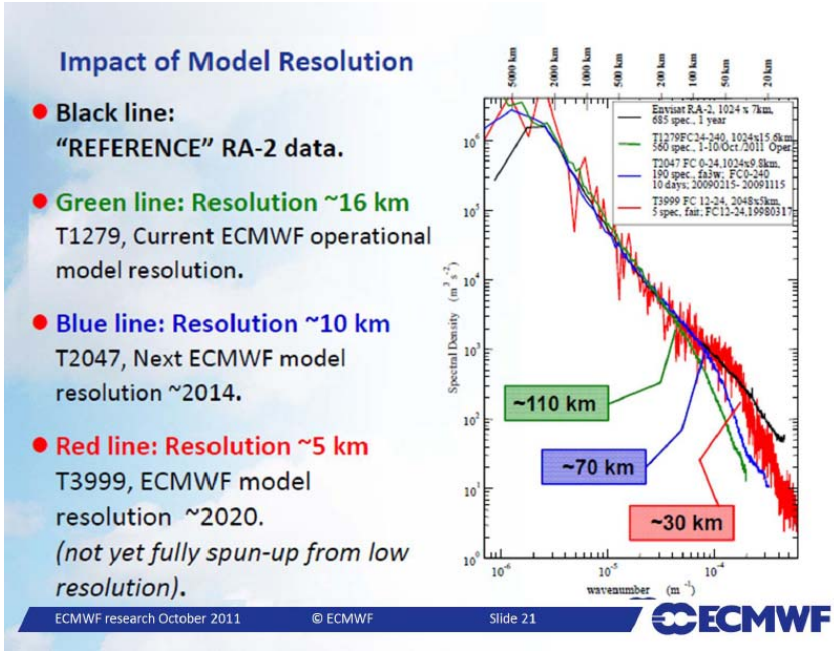

Figure 3.6: The spectral density of the operational ECMWF model (green) and two versions of the ECMWF model planned for the future (blue and red) compared to spectral densities of the Envisat RA-2 satellite data (black). Note that the ECMWF operational forecasting model (16 km grid spacing) starts deviating from the satellite data at an effective horizontal resolution of about 110 km (source: Källén, 2011).

The important question when estimating wind energy production is what this means for the quality of spectral model wind data. Houchi et al (2010) compared high resolution radiosonde wind profiles up to about 30 km altitude to collocated operational ECMWF 12 hour short range[31] forecast winds. The probability distributions of the modelled and observed horizontal winds were very similar at most levels (figure 3.7). At the lowest height (around 1 km), only the highest wind speeds were underestimated by the ECMWF model (the 90% percentile zonal wind speed[32] of the radiosondes is greater than that of ECMWF) and these high wind

[29] Numerical instability of weather forecasting models is caused by round-off or truncation errors when they grow exponentially.
[30] Spectral models solve the primitive meteorological equations by applying a Fourier analysis of the spatial patterns.
[31] Short range forecasting: from12 up to 72 hour forecasts of weather parameters (http://www.wmo.int/pages/prog/www/DPSdev/GDPS-Supplement5-AppI-4.html)
[32] The zonal wind speed is the east-west component of the horizontal wind vector.

speeds are not important for power production. Summing up, the consequences of using diffusion operators in spectral weather forecasting models for the purpose of quantifying wind energy production are unimportant.

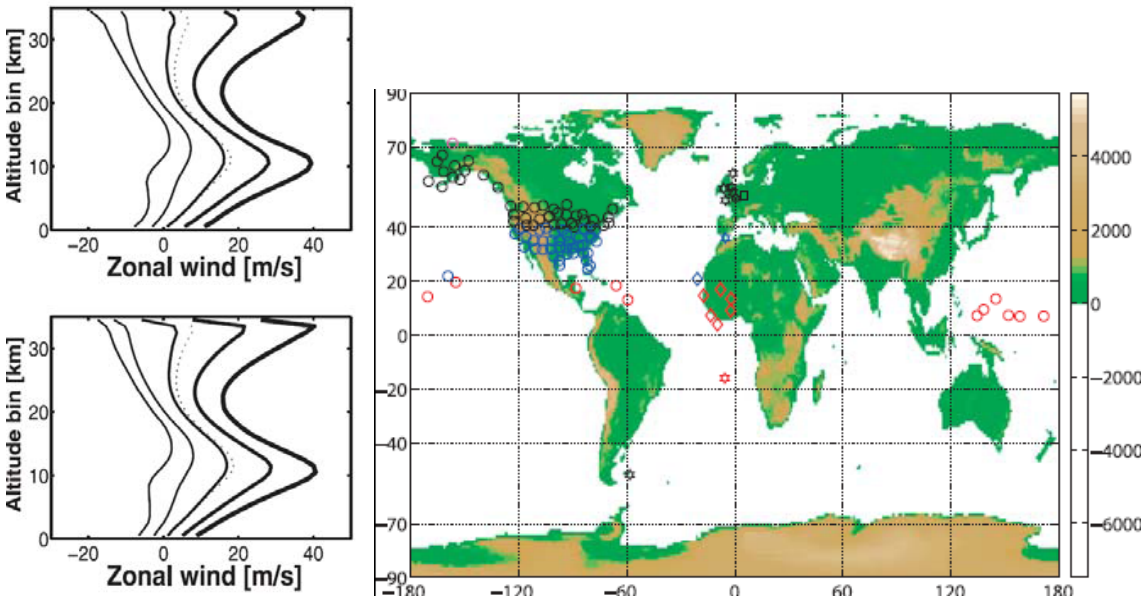

Figure 3.7 Zonal wind speed statistics for the Northern Hemisphere Mid-Latitude climate region (40-70°) based on high resolution SPARC[33] 12 sec (≈ 60 m) radiosonde measurements collocated with ECMWF 12 hour short range forecasts. In the upper graph (left panel) the measured statistics, in the lower graph the modelled ones. The dotted line is the average, the other 5 are percentiles (10, 25, 50, 75 and 90%) of the wind speed frequency distribution at the given height. In the map of the world (right panel) the black circles show the geographical locations of the SPARC radiosonde stations in the Northern Hemisphere Mid-Latitude climate region (source: Houchi, 2010).

3.2.2 Vertical resolution and range

Vertical model levels of ERA interim and the operational version of ECMWF are not expressed in meters, but in "sigma-levels". In the lower and mid troposphere they follow the earth's surface and in the upper stratosphere and mesosphere they are surfaces of constant pressure. ERA Interim uses 60 levels with the model top at 0.1 hPa and the operational ECMWF model (used in this report) 91 levels with the model top at 0.01 hPa. In the lowest 15 km of the atmosphere the vertical resolution of the operational ECMWF model is higher (figure 3.8).

The study by Houchi et al (2010) showed that the probability distributions of the modelled and observed horizontal winds were very similar at most levels (figure 3.7), but the

[33] Where the SPARC high resolution radiosonde wind profiles are mainly in the USA, other also high resolution radiosonde wind profiles are available in our region: six in the UK with a vertical resolution of 10 m (BADG) and one with a vertical resolution of 50 m (De Bilt).

distributions of vertical wind speed shear (change in wind speed per metre of height) were substantially underestimated by the model (not shown).

Figure 3.8 shows a comparison for a single radiosonde flight. The comparison is not a fair one because: (a) 12 hour ECMWF forecast is used for the comparison, not the ECMWF analyses, (b) the time averaging of the radiosonde (6 seconds) is not the same as that of ECMWF (≈ 20 minutes) and (c) the lowest 200 m ECMWF is verified with measurements of nearly 2 hours earlier. The model averages out the fine structure captured by the radiosonde because the model grid-boxes are large compared to the turbulent eddies causing the fine structure. As figure 3.7 showed, the model does describe the frequency distribution of the wind speed correctly. The model does less well when it comes to describing the wind shear. Wind shear is large when the atmospheric stability is stable. The effect of wind shear on wind energy production is not well understood and studies show that the effect is under some circumstances positive and under others negative (see the last paragraph of section 1.1.1).

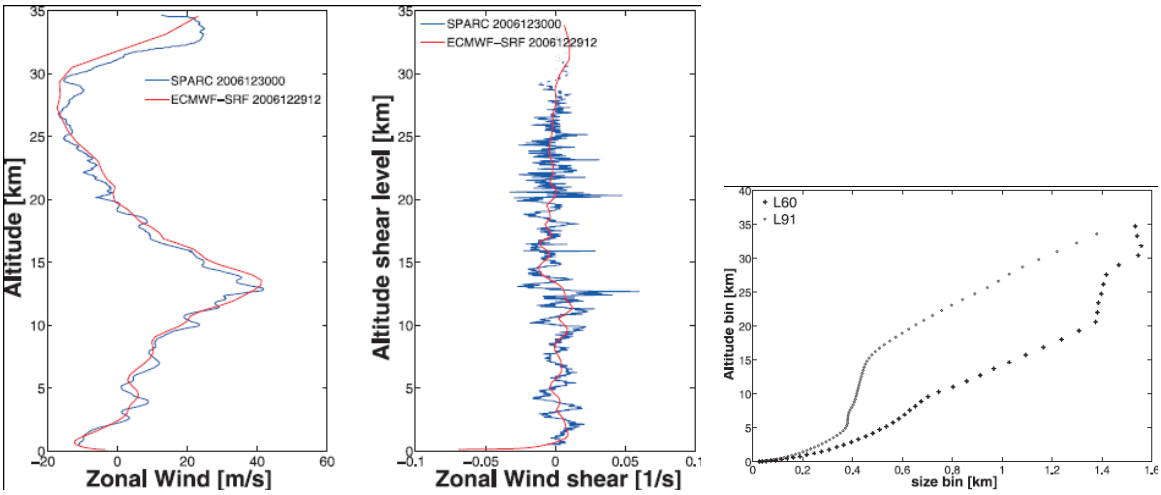

Figure 3.8 High resolution radiosonde (SPARC with a vertical resolution of 30 m ≈ 6 sec) collocated with an independent L91 ECMWF short-range forecast at 90.1W 32.3N on 30-12-2006 00 UTC (left and middle graphs). The model describes the general shape of the wind profile, but cannot possibly describe the fine structure captured by the 6 second radiosonde measurements. The netto effect of such small scale variations on the wind turbine rotor and over a number of years is unlikely to have a large effect on estimates of annual wind energy production. The L91 version of ECMWF was used between 02-02-2006 and 25-06-2013 and has an enhanced number of vertical levels in the first 15 km compared to the L60 version that was used before (right graph) (source: Houchi, 2010).

Hub heights of modern wind turbines are typically between 80 m on land (figure 3.9) and 120 m offshore. With rotor diameters between 80 m on land (figure 3.9) and 180 m offshore and assuming the smallest rotor diameter belongs to the wind turbine with the lowest hub height and vice versa, this implies that wind information is required between 40 m *(80-40)* and 210 m *(120+90)*. Only the European wind atlas gives information up to a level of 200 m, but the information above 100 m is of limited value (pg 20 Troen et al, 1989). Existing wind atlases provide information at heights as follows:

- European wind atlases at 10, 25, 50, 100 and 200 m above sea level
- KEMA/Senternovem atlases at 80, 100 and 120 m
- OWA-NEEZ atlas at 40, 90 and 140 m
- NORSEWInD: Envisat ASAR maps at 10 and 100 m

- NORSEWInD: QuikSCAT and ASCAT coastal L3 wind product maps at 10 m
- NORSEWInD: SSM/I wind power index trends based on wind speeds at 100m

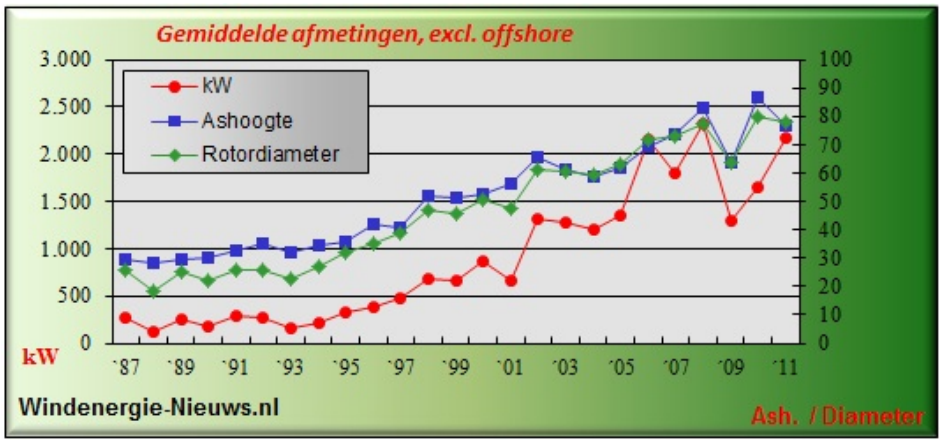

Figure 3.9 Trend in hub height (blue) and rotor diameter (green) for Dutch wind turbines on land (source: http://www.windenergie-nieuws.nl/statistieken-gemiddelde-afmetingen-onshore-in-nederland/).

3.3 Stability parameterisation

Most available wind atlases and maps are based on observations at 10 m or at the sea surface (satellite observations). They provide information on the spatial variability of the wind climate, but for wind energy purposes these observations have to be extrapolated to higher levels in the atmosphere, which means that assumptions have to be made on the influence of atmospheric stability on the vertical wind profile. This implies that the vertical wind profile will contain errors, but as long as the estimate of the climatological average frequency distribution is realistic at wind turbine hub height (around 120 m these days for offshore installations) a good estimation of the wind energy production can be made. Even that remains a challenge.

For the WASP-based maps (European wind atlases and KEMA-SenterNovem) wind mast measurements at 10 m are transformed into geostrophic winds assuming neutral stability and then transformed back to 10 m for 4 standard roughness classes, again assuming neutral stability. This means that any deviation from the logarithmic wind profile due to stability effects in the earlier transformation from 10 m wind to geostrophic wind is compensated for. In order to calculate the wind parameters at higher levels (25, 50, 100 and 200 m), one stability modification is applied to the logarithmic wind profile to obtain an estimate of the climatological average wind profile[34]. This modification depends on the climatological average and root-mean-square of the surface heat flux (one value for land, one for sea). One of the formulas used to do this includes the Ψm-function which describes the modification of the logarithmic wind profile due to (un)stability of the atmosphere. The Ψm-function is an empirical function that has been improved since the release of the WASP-based maps. The Beljaars/Holtslag stability function (formula 1.11) is the best one currently available for stable conditions (Sharan et al, 2003). For unstable conditions, Peña (2012) found that the

[34] WAsP does not work with 10 min or hourly data so the Ψm-function can only be applied to the average wind profile (Cleijne, DNV GL, former KEMA)

highest correlation between the extrapolated wind speeds and the observations (LIDAR and wind masts) was achieved by adapting the traditional Businger-Dyer formula (formula 1.3a) to take into account the height of the Planetary Boundary Layer (PBL, formula 2.1e) and using the NORSEWInD Ψm-function of formula 1.12a .

The numerical computer models used for weather forecasting also face the challenge of how to represent the processes in the boundary layer accurately. Traditionally these models were tuned to optimise the model winds at the standard measurement height of 10 m, but as the demand for wind forecasts and climatology at wind turbine hub-height increases, it becomes more important to verify the models at these higher levels too. Unfortunately, there are few tall wind masts, especially at sea, and none of the masts at sea are 200m high. The offshore tall wind masts on the southern North Sea are: the OWEZ (or EAZ) mast with measurements at 21, 70 and 116 m, the FINO1 mast with measurements at 33, 40, 50, 80, 90 and 100 m and the Greater Gabbard mast with measurements at 42.5, 52.5, 72.5, 82.5 and 86.5 m (figure 2.6). For the NORSEWInD project LIDAR's[35] were installed which are able to measure wind profiles at higher levels (up to 300 m). Another option is using Large Eddy Simulations (LES) to verify PBL parameterisations in weather forecasting models. In LES models turbulence equations are solved, not parameterised as is done in traditional models[36].

Adapted Businger-Dyer formula:

$$u(z) = u_*/\kappa \, [\, \ln(100/z_o) - \psi(100/L) * (1-100/2PBLH) \,] \qquad (2.1e)$$

- PBLH = Planetary boundary layer height from WRF
- Stability function ψ_m according to formula 1.12:

Best ψ_m-function for stable conditions (Beljaars/Holtslag, 1991):

$$-\psi_m = a\, z/L + b\,(z/L - c/d)^{-d\, z/L} + bc/d \qquad \text{(stable conditions } z/L > 0) \qquad (1.11)$$

- a = 0.7
- b = 0.75
- c = 5
- d = 0.35
- z/L small: ψ_m behaves like $\psi_m = -5\, z/L$ (= Businger-Dyer)
- z/L large: $-\psi_m \approx a\, z/L$

Best ψ_m-function for unstable conditions (NORSEWInD, 2012):

$$\psi_m = 3/2 \ln [\, (1 + x + x^2) / 3 \,] - \sqrt{3} \arctan [\, (2x+1) / \sqrt{3} \,] + \pi / \sqrt{3}$$

$$\text{where } x = [\, 1 - 12\, (z / L) \,]^{1/3} \qquad (\text{unstable conditions } z/L \leq 0) \qquad (1.12a)$$

[35] LIDAR is a remote sensing technology that measures distance by illuminating a target with a laser and analyzing the reflected light. A doppler LIDAR can be used to measure temperature and/or wind speed.
[36] This is the case for length scales larger than grid-spacing. Turbulence on length scales smaller than grid-spacing are still parameterised: this occurs regularly under stable atmospheric conditions.

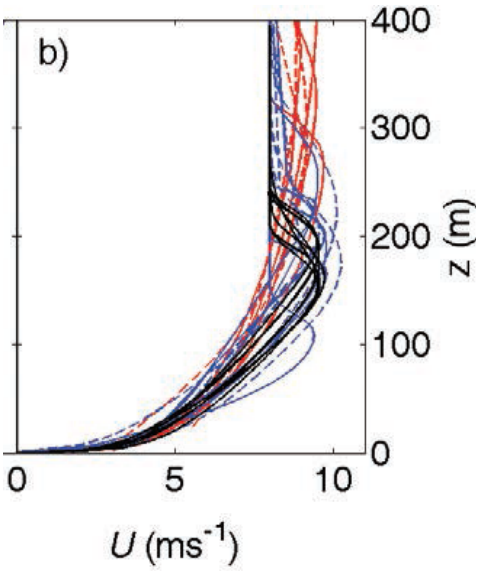

Figure 3.10: Modelled vertical profiles of the horizontal wind speed (m/s) when the boundary layer is extremely stable (Artic conditions are simulated. The red lines are the SCM versions (Single Column Model) of the operational weather forecasting models, blue lines SCM versions of the research models and black lines the Large Eddy Simulations (LES). Under these extreme conditions, the operational models exhibit too much vertical diffusion and too little vertical shear compared to LES and the research models (source: Holtslag, 2013)

In an attempt to evaluate the boundary layer parameterisations in the models currently in use at the operational weather forecast and climate centres (including ECMWF), Holtslag et al (2013) compared single column versions (SCMs[37]) of these models to observations (e.g. Cabauw) and ensembles of fine-scale LES models. Figure 3.10 shows that, in the extremely stable conditions encountered at the Artic, SCMs of the operational models (red) exhibit too much vertical diffusion and too little vertical shear. This leads to an underestimation of the wind speed at heights which are interesting for wind energy (40-200 m) and overestimation of the depth of the boundary layer compared to the black LES reference values (latter not shown). Figure 3.11 (BL summer school Les Houches, 2008) shows that reducing the vertical diffusion can improve the model skill for higher level wind speeds. For 3 days in July 1987 a comparison is made between ERA40[38] on a 126 km grid (with the same vertical diffusion scheme as ERA-Interim that is used for the wind atlas presented in chapter 4) and Cabauw measurements. In the nights where the atmosphere is stable a clear improvement of the 200 m model wind (compared to observations in black) can be seen if vertical diffusion in the model is reduced (blue line compared to red/green).

[37] SCM is essentially the column physics of an atmospheric model considered in isolation from the remainder of the atmospheric model
[38] Reanalyses model ERA40 was the predecessor of ERA-interim

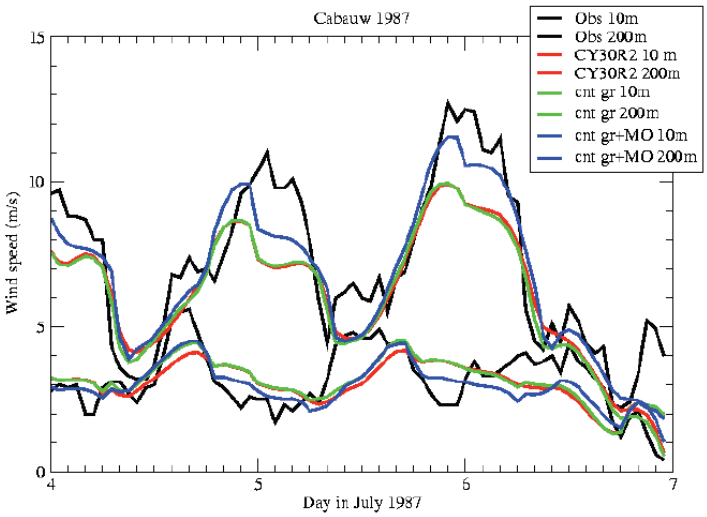

Figure 3.11: comparison between ERA40 (red), modified ERA40 allowing counter gradients (green), modified ERA40 allowing counter gradients and with less vertical diffusion (blue) and Cabauw measurements (black) for 3 days in July 1987 (source: BL summer school, Les Houches, 2008)

Sandu et al (2013) compared ECMWF (on a 16 km grid, the same grid-spacing as the one from the ECMWF version used for the wind atlas presented in chapter 4) to the 2011 annual average diurnal cycle at Cabauw. In the evening and night when the atmosphere is on average stable, the wind speed at 80 and 200 m is clearly underestimated by ECMWF (figure 3.12) and at 10 m slightly overestimated. During the day (on average unstable) the opposite applies and over the whole 24 hours the errors cancel each other out to some extent.

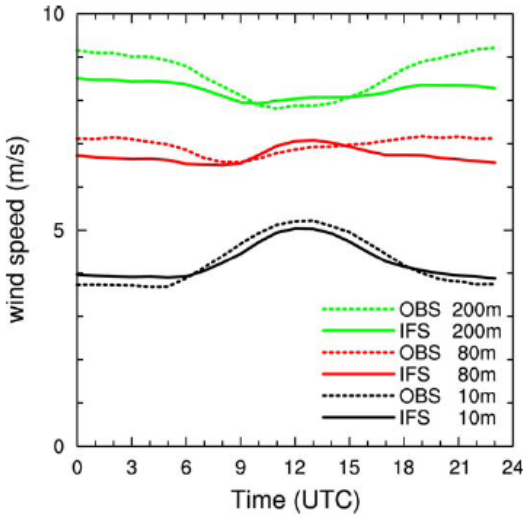

Figure 3.12: ECMWF IFS (deterministic T1279 L91 run, cycles 37r2 and 37r3) daily 00 UTC forecast (lead times 24-42 h) compared to 2011 annual average diurnal cycle at Cabauw at 10, 80 and 200 m height (source: Sandu, 2013).

The angle between the surface wind and the geostrophic wind is directly related to depth of the turbulent boundary layer such that deeper boundary layers have smaller wind direction differences (and shallower boundary layers larger angular differences). So, if operational models overestimate the depth of the boundary layer, they underestimate the angle between the surface wind and the geostrophic wind: in the lowest levels of the atmosphere the wind is

not sufficiently backed[39]. Figure 3.13 shows this model bias compared to QuikSCAT for ECMWF wind direction.

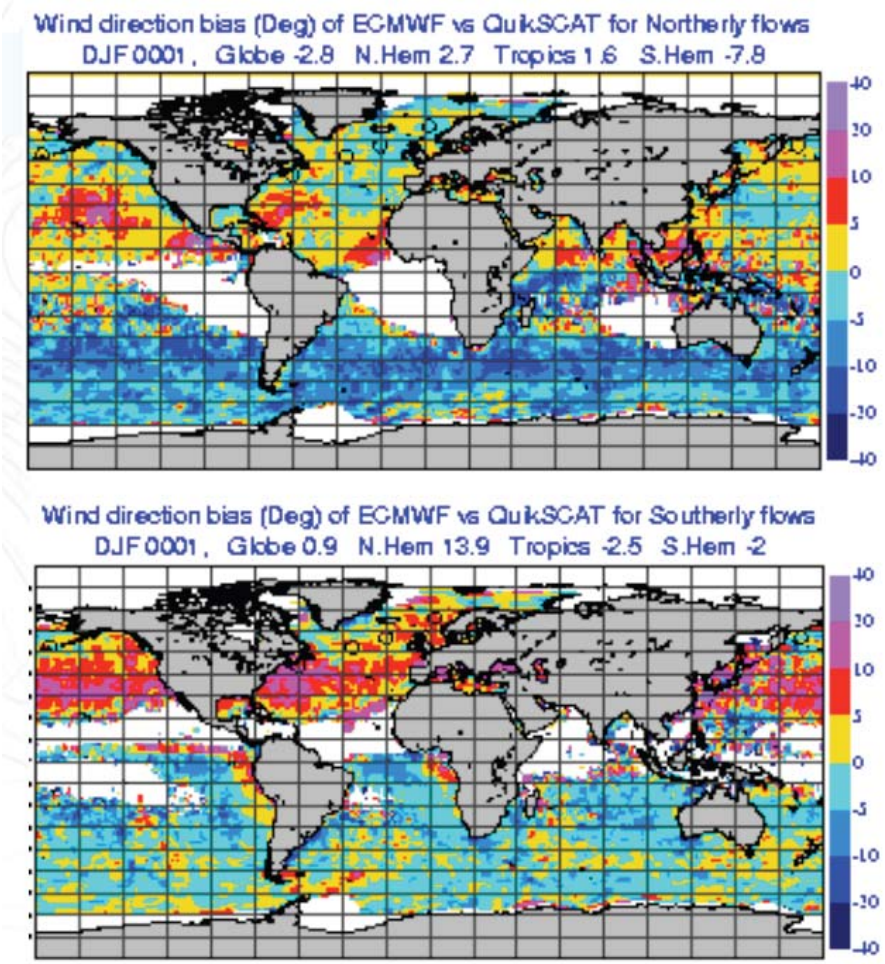

Figure 3.13 Wind direction bias of ECMWF short range forecast for 10m winds relative to QuikSCAT surface winds for December, January and February: positive values indicate that model winds are rotated clockwise compared to observed winds. So on the North Sea ECMWF does not back the wind at the surface enough by 0-5^{o} for northerly flows and by 5-10^{o} for southerly flows. Only for wind speeds of at least 4 m/s (source: Brown, 2005)

So, most state-of-the-art operational weather forecasting and climate models have problems with the representation of wind profiles in stable conditions and these problems can not easily be solved (reducing the vertical mixing in the model has negative consequences for the quality of the medium range[40] 10 m wind forecasts). Although the atmosphere offshore is less often stable than the atmosphere on land, stable stratification does occur regularly at sea (figure 3.13 and 3.14 which compares the Harmonie weather forecasting model to tall tower wind speed measurements) and will contribute to the offshore wind climate, especially for

[39] Due to friction the wind is not only decreasing with height, but also backing (wind direction is "turning" anti-clockwise as seen from above). If the wind is veering, wind direction is "turning" clockwise.

[40] Medium range forecasting: beyond 72 hours and up to 240 hours description of weather parameters (http://www.wmo.int/pages/prog/www/DPSdev/GDPS-Supplement5-AppI-4.html)

coastal areas where the water cools down most in winter (increasing the chance of stable stratification) and where the influence of the higher roughness of the land is felt when the wind is blowing from land to sea. Figure 3.12 shows that the ECMWF operational model underestimates the 80 m wind speed in stable conditions above land (Cabauw). Figure 3.14 shows that for winter months Harmonie's underestimation of the 80 m wind (compared to the wind at 40 m) is less at sea (FINO) than above land (Cabauw): about half as much. If we assume that the same is true for ECMWF, then the 0.5 m/s underestimation at Cabauw implies an underestimation of about 0.25 m/s at sea. Sathe (2010) showed that stable conditions at the Egmond-aan_Zee mast occur about half of the time in winter and only 20 % of the time annually. Furthermore, Sathe also shows that, just as above land, stable conditions occur mainly at low wind speeds that are less important for wind energy production. The effect of the underestimate during stable conditions on the annual average wind energy production is therefore likely to be small. However, a more precise quantification of the model error in stable conditions and how it would affect the annual average wind energy production is not well understood and will depend upon the exact interplay of stability effects at different heights, the distance from the coast, the size and height of the wind turbine rotor in question and other dependencies (see the discussion of the last paragraph of section 1.1.1).

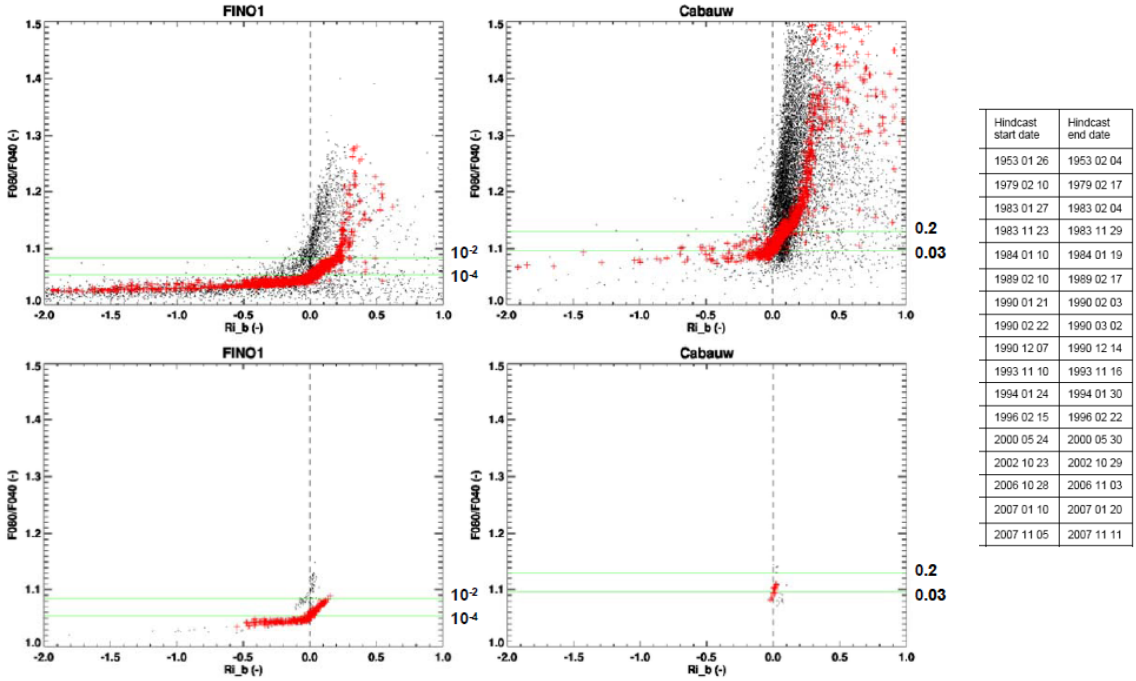

Hindcast start date	Hindcast end date
1953 01 26	1953 02 04
1979 02 10	1979 02 17
1983 01 27	1983 02 04
1983 11 23	1983 11 29
1984 01 10	1984 01 19
1989 02 10	1989 02 17
1990 01 21	1990 02 03
1990 02 22	1990 03 02
1990 12 07	1990 12 14
1993 11 10	1993 11 16
1994 01 24	1994 01 30
1996 02 15	1996 02 22
2000 05 24	2000 05 30
2002 10 23	2002 10 29
2006 10 28	2006 11 03
2007 01 10	2007 01 20
2007 11 05	2007 11 11

Figure 3.14 Observed (black) and modelled (red) 80 m/40 m wind speed ratio for FINO1(at sea) and Cabauw (land station). Top panels: observations for all available winter months (December, January and Februari) in the period 2004-2009 and Harmonie model data for all hindcast periods except for the first one in the list: the 1953 storm. Bottom panels: the same but only for10 m wind speeds exceeding 17.2 m/s (8 bft). Ri_b is the Bulk Richardson number which indicates whether the atmosphere is unstable (Ri_b < 0), neutral (Ri_b > 0) or stable (Ri_b > 0). Horizontal green lines indicate 80/40 wind speed ratios corresponding to neutral atmosphere and specific roughness lengths as indicated along right axis (10^{-2} and 10^{-4} at sea and 0.03 and 0.2 on land) (source: Baas, 2014).

3.4 Roughness parameterisation

The roughness information which is used to make the European wind atlases is based on paper maps from 1970-1976 and the roughness information for the KEMA-SenterNovem map on satellite images of 1995-1997. For wind atlases on land, an update of the roughness information would be useful as the past 30-50 years have seen a stilling of the 10 m wind speed over land as a result of an increase in the surface roughness caused by changes in land-use including urbanization, forestation, and a decrease in pasture land area (Wever, 2012), Vautard, 2010 and Kattenberg, 2013).

Knowledge about roughness at sea has evolved since WAsP, where the roughness length at sea is assumed to be a constant of 0.0002 m which was assumed to be "just as good as Charnock[41] with a constant of 0.014 for moderate to high wind speeds". If there is more drag, the wind at the surface will be less and there will be a stronger increase in wind speed with height (and vice versa). Therefore, the parameterisation of the drag coefficient will have an effect on the wind speed at the levels we are interested in (between 40 and 200m). The question is whether this has important consequences for wind energy production estimates. In the first version of the OWA-NEEZ wind atlas (40, 90 and 140 m) described in section 2.2, the sea surface roughness only depended on wind speed (Charnock relation), but in the second version the sea surface roughness is a function of wave steepness too. The accuracy of the Weibull shape parameter was only improved by 1% - 2%. In the light of this evidence, the improvements in the modelling of the drag relation would seem to have no great importance for wind energy production estimates. This conclusion is however tentative and further research is required before harder conclusions can be drawn.

[41] Charnock's model (1955) relates the roughness length to the friction velocity. The Charnock constant in the formula is site specific and often assumed to be 0.032 for The North Sea and 0.018 for Lake IJssel.

Recommendations

Based on the findings presented in this report, we recommend making a high resolution wind atlas for the North Sea that includes information on the long-term variability of the wind climate, provides information up to at least 200 m height and can reproduce more than just a climatological average of stability effects on the wind profile. In part 2 of this report we present a wind climatology which meets all these requirements. It is based on reanalyses model ERA-Interim (to ensure that long-term variability is included) and operational atmospheric weather forecasting model Harmonie (to enhance the resolution). At this stage it is no more (or less) than model climatology and validating against observations is still needed. Therefore validation will be the main recommendation for part 2 of this report.

References

(For part 1 and 2 of the report)

- Baas, P. and H.W. van den Brink (2013) Evaluation of Harmonie simulations for 16 historical storms. Contribution to the WP1 of the WT12017_HB Wind Modelling Project.
- Baas, P. and H.W. van den Brink (2014) The added value of the high-resolution Harmonie model for deriving HBC's. Contribution to the WP1 of the WT12017_HB Wind Modelling Project.
- Bakker A.M.R. and Van den Hurk B.J.J.M. (2011) Estimation of persistence and trends in geostrophic wind speed for the assessment of wind supply in Northwest Europe, Clim. Dyn. doi 10.1007/s00382-011-1248-1
- Bay Hasager C., Badger M., Mouche A., Stoffelen A., Driesenaar T., Karagali I., Bingöl F., Peña A., Astrup P., Nielsen M., Hahmann A., Costa P., Berge E. and R. Erland Bredesen (2012). NORSEWInD satellite climatology. DTU Wind Energy-E-0007(EN)
- Beljaars, A.C.M. (2008) Wind and Stability. BL summer school, Les Houches Jun-2008
- Beljaars, A.C.M and A.A.M. Holtslag (1991). Flux Parameterization over Land Surfaces for Atmospheric Models. J. Appl. Meteor., 30, 327-341.
- Berge, E., Byrkjedal, O., Ydersbond, Y., & Kindler, D. (2009). Modelling of offshore wind resources. Comparison of a meso-scale model and measurements from FINO-1 and North Sea oil rigs. *In proceedings of EWEC2009 Marseille, March 2009.*
- Bidlot J.R., Janssen P. and S. Abdalla (2007). Impact of the revised formulation for ocean wave dissipation on the ECMWF operational wave model. Tech. Memo. 509, ECMWF: Reading, UK.
- Brown, A.R., A.C.M. Beljaars, H. Hersbach, A. Hollingsworth, M. Miller and D. Vasiljevic ((2005). Wind turning across the marine atmospheric boundary layer, Q.J.R. Meteorol.Soc. (2005), 131, pp. 1233-1250, doi 10.1256/qj.04.163
- Caires, S, H. de Waal, J. Groeneweg, G. Groen, N. Wever, C. Geertse and M. Bottema (2012). Assessing the uncertainties of using land-based wind observations for determining extreme open-water winds. Journal of wind engineering nov 2012
- Giebel, G. and Gryning, S (2004). Shear and stability in high met masts, and how WAsP treats it. Proceedings. Delft : Delft University of Technology, 2004. p. 356-363.
- Högström, U. L. F. (1988). Non-dimensional wind and temperature profiles in the atmospheric surface layer: a re-evaluation. Bound. Layer Meteorology, 42, 55-78.
- Holtslag, A.A.M, G. Svensson, P. Baas, S. Basu, B. Beare, A.C.M. Beljaars, F.C. Bosveld, J. Cuxart, J. Lindvall, G.J. Steeneveld, M. Tjernström and B.J.H. van de Wiel (2013). Stable atmospheric boundary layers and diurnal cycles: challenges for weather and climate models. Bull. Amer. Meteor. Soc., 94, 1691–1706. doi: http://dx.doi.org/10.1175/BAMS-D-11-00187.1
- Houchi K., A. Stoffelen, G.J. Marseille and J. de Kloe (2010). Comparison of wind and wind shear climatologies derived from high-resolution radiosondes and the ECMWF model. J. Geophys. Res., D, 2010, 115**,** 22123, doi: 10.1029/2009JD013196

- Källén, E. (2012). ECMWF forecasting system - research and development. Presentation at the15th workshop on use of High Performance Computing (HPC) October 2012: http://www.ecmwf.int/newsevents/meetings/workshops/2012/high_performance_computing_15th/Presentations/pdf/Kallen.pdf
- Kattenberg, A., Verver, G., Homan, C.D., Jilderda, R., Leander, R., Wijnant, I.L. and Stepek, A (2013) Klimaatbestendig Schiphol Syntheserapport HSMS02. KvK nr. KvK99/2013, ISBN 978-94-90070-69-4
- Karagali I, A. Peña, M. Badger and C. Bay Hasager (2012) Wind characteristics in the North and Baltic Seas from the QuikSCAT satellite wileyonlinelibrary.com. DOI: 10.1002/we.1565
- Lettau, H. (1969). Note on aerodynamic roughness-parameter estimation on the basis of roughness-element distribution. J. Appl. Met. 8, 828-832.
- Marseille, G.J., Stoffelen, A., Schyberg, H., Megner, L., Kornich H. (2013) *VHAMP: Vertical and Horizontal Aeolus Measurement Positioning* ESA contract reports
- Peña A., Mikkelsen T., Gryning S.E., Hasager, C. B., Hahman A. N., Badger M., Karagali I. and M. Courtney (2012). Offshore vertical wind shear. DTU Wind Energy-E-Report-0005(EN)
- Rareshide E, Tindal A, Johnson C, Graves A M, Simpson E, Bleeg J, Harris T and Schoborg D (2009). Effects of complex wind regimes on Turbine Performance. Proceedings American Wind Energy Association WINDPOWER Conference (Chicago, IL)
- Ricciardulli (2013) http://coaps.fsu.edu/scatterometry/meeting/docs/2013/CalValClim/Ricciardulli_Wentz_ovwst_2013_wind_diurnal.pdf
- Sandu I, A. Beljaars, P.Bechthold, T. Mauritsen and G. Balsamo (2013). Why is it so difficult to represent stably stratified conditions in numerical weather prediction (NWP) models? Journal of advances in modelling earth systems, vol. 5, 117-133, doi: 10.1002/jame.20013, 2013
- Sathe, AR (2010). Atmospheric stability and wind profile climatology over the north sea - case study at Egmond aan Zee. In S Voutsinas & T Chaviaropoulos (Eds.), *Proceedings of the conference torque 2010 The science of making torque from wind* (pp. 1-10). Athens, Greece: EAWE / EWEA.
- Sharan, M. and S.G. Gopalakrishnan (2003). Mathematical Modelling of Diffusion and Transport of Pollutants in the Atmospheric Boundary Layer. Pure applied geophysics, 160 (2003) 357-394. 0033-4553/03/020357-38Troen, I. and E.L. Petersen (1989). *European Wind Atlas*. Risø National Laboratory, Roskilde. 656 pp. ISBN 87-550-1482-8.
- Sousa, M. C., I. Alvarez, N. Vaz, M. Gomez-Gesteira, J. M. Dias, 2013: Assessment of Wind Pattern Accuracy from the QuikSCAT Satellite and the WRF Model along the Galician Coast (Northwest Iberian Peninsula). *Mon. Wea. Rev.*, **141**, 742–753. doi: http://dx.doi.org/10.1175/MWR-D-11-00361.1
- Troen, I. and E.L. Petersen (1989). European Wind Atlas. ISBN 87-550-1482-8. Risø National Laboratory, Roskilde. 656 pp.
- Vautard R, Cattiaux J, Yiou P, Thépaut JN and Ciais P (2010), Northern Hemisphere atmospheric stilling partly attributed to an increase in surface roughness, Nature Geoscience 3 (11), 756-761, doi:10.1038/ngeo979.

- Verkaik, J. (2003) A method for the geographical interpolation of wind speed over heterogeneous terrain. Technical Report KNMI-HYDRA 11-12, Koninklijk Nederlands Meteorologisch Instituut.
- Vogelzang, J., A. Stoffelen, A. Verhoef and J. Figa-Saldana (2011) *On the quality of high-resolution scatterometer winds* J. Geophys. Res., 2011, **116**, C10033, doi:10.1029/2010JC006640.
- Wagner R, Antoniou I, Pedersen S M, Courtney M S and Jorgensen H E (2009). The influence of the wind speed profile on wind turbine performance measurements. Wind Energy 12, 348-62
- Weill, A. Eymard, L. Caniaux, G. Hauser, D. Planton, S. Dupuis, H. Brut, A. Guerin, C. Nacass, P. Butet, A., Cloche, S., Pedreros, R., Durand, P., Bourras, D., Goirdani, H., Lachaud, G. and G. Bouhours (2003). Toward a better determination of turbulent airsea fluxes from several experiments. J. Climate, 16, 600-618.
- Wever, N. (2012), Quantifying trends in surface roughness and the effect on surface wind speed observations. J. Geophys. Res., 117, D11104, doi:10.1029/2011JD017118.
- Wharton S and Lundquist J K (2012). Atmospheric stability affects wind turbine power collection. Environ. Res. Lett. 7, 014005 (9pp)

Acknowledgements

We thank Ad Stoffelen (KNMI), Peter Baas (KNMI), Hans Cleijne (DNV GL) and Alfredo Pena Diaz (WAsP-support) for their comments and help.

Appendix 1: Project Plan

Noordzee windklimatologie op hoogte t.b.v. sturing energiebeleid van IenM

Profijtbeginselproject (deelopdracht structuurvisie wind op zee) voor DGRW

Projectgroep:
Ine Wijnant (projectleider/rapportage), Henk van den Brink en Andrew Stepek (windklimatologie kaarten), Gerrit Burgers (assistent projectleider), Gertie Geertsema (advies)
Opdrachtgevers:
Nathalie de Koning en Frank Stevens van Abbe
Budget en doorlooptijd:
32.000 euro en half jaar
Plan van aanpak (wat willen we doen en waarom zo):

Gebruik modellen i.p.v. waarnemingen:

Er zijn weinig waarnemingen op hoogte op de Noordzee. Daarom willen we voor het bepalen van de windklimatologie op 120 m hoogte gebruik maken van weermodellen. Het voordeel van deze modellen is dat ze een 100% dekking van het gebied geven en bovendien een fysisch onderbouwd beeld geven van de verticale opbouw van de atmosfeer (stabiliteit). Een nadeel is dat de oppervlakteruwheid niet afhankelijk is van de windrichting, maar een gemiddelde is over de kleinste gebiedsgrootte ("gridbox") van het model. Boven zee is dit nadeel echter alleen significant op afstanden van de kust die kleiner zijn dan de kleinste roosterpuntsafstand ("horizontale resolutie") van het model.

Lange reeksen en hoge resolutie:

Bakker* heeft een studie gedaan naar de wind op de Noordzee en heeft op basis van drukmetingen een geostrofische windreeks van 140 jaar gecreëerd. Deze reeks laat zien dat een periode van ruim 40 jaar nodig is om de volledige jaar op jaar variatie van de (geostrofische) windsnelheid van de hele periode (140 jaar) te bemonsteren. Het enige model waarmee we een dataset van dichtbij 40 jaar windinformatie kunnen genereren is ERA-Interim (34 jaar). Nadeel van ERA-Interim is echter de vrij lage horizontale resolutie (80 km). Daarom zijn we van plan om ook de operationele ECMWF uitvoer (resolutie 16 km) van de afgelopen 2 jaar te gebruiken om de uiteindelijke kaarten te maken (langer dan 2 jaar kan niet, omdat er dan te grote wijzigingen zijn in het model). Door een statistische relatie te leggen tussen de operationele ECMWF winduitvoer en die van ERA-Interim, kunnen we klimatologische kaarten leveren met een resolutie van 16 km.

Beperkt geldig voor de territoriale wateren:

Met een horizontale modelresolutie van 16 km blijven de kaarten beperkt geldig voor het gebied tot 16 km uit de kust omdat het model daar de oppervlakteruwheid van de zee middelt met die van het land. Aangezien windparken op dit moment gerealiseerd worden buiten de territoriale wateren (meer dan 22 km uit de kust), is dat geen probleem (alle modelpunten hebben daar uitsluitend de zeeruwheid). Mocht het beleid op dit punt wijzigen, wordt dat wel een punt van aandacht.

Inhoud kaarten:

Naast kaarten met de klimatologisch gemiddelde windsnelheid, stellen wij voor ook de twee Weibullparameters (vormparameter, k en schaalparameter, λ uit onderstaande formule voor de frequentieverdeling van de windsnelheid, x) voor elk model gridpunt op de Noordzee te berekenen. M.b.v. een standaard windturbine power curve is op basis van deze gegevens de windenergie opbrengst uit te rekenen.

$$F(x;\lambda,k) = 1 - e^{-(x/\lambda)^k}$$ (Weibull verdeling)

Naast de gemiddelde windsnelheid en de Weibullparameters, is het belangrijk om per roosterpunt op de Noordzee informatie te geven over de variabiliteit van de wind, bijvoorbeeld het maximum en het minimum van het 10 jaar lopend gemiddelde. Aangezien de financiering van windparken vaak gebeurt op basis van een conservatieve raming van de 10 jaar gemiddelde windsnelheid en verdeling, is het interessant om de laagste 10 jaar gemiddelde windsnelheid met een kans van optreden van bijvoorbeeld 10% te geven.
Op verzoek van DGRW leveren we ook de eens in de 50 en eens in de 100 jaar extremen, een windroos met windrichtingverdeling, een kaart met windsnelheden die gestandaardiseerd zijn op de standaard luchtdichtheid en (indien tijd en budget het toelaat) een beperkte vergelijking met OWA-NEEZ.

De operationele ECMWF run geeft een standaarduitvoer op 100m, en op sigma levels (percentages van de luchtdruk op gemiddelde zeeniveau). Wij leveren de gegevens aan op sigmalevels overeenkomend met 40, 60, 80, 100, 120, 140, 160, 180 en 200 m.

Rapportage:

Rapportage is in het Engels. In het rapport zal naast een inleiding over bestaande windkaarten op hoogte (met hun nut en beperkingen), een uitgebreide beschrijving gegeven worden van de methode waarop de kaarten in dit project gemaakt zijn en hoe ze gebruikt dienen te worden. Verder zullen aanbevelingen gedaan worden voor verificatie en verbetering van de kaarten (bijvoorbeeld met gegevens van de OWEZ meetmast, scatterometer data die gebruikt is in het NorseWind project of hindcast HARMONIE modeluitvoer op 2.5 km resolutie).

[*] Bakker AMR and Van den Hurk BJJM (2011) Estimation of persistence and trends in geostrophic wind speed for the assessment of wind supply in Northwest Europe, Clim. Dyn.(accepted). DOI 10.1007/s00382-011-1248-1

A complete list of all KNMI-publications (1854 – present) can be found on our website

www.knmi.nl/knmi-library/knmipub_en.html

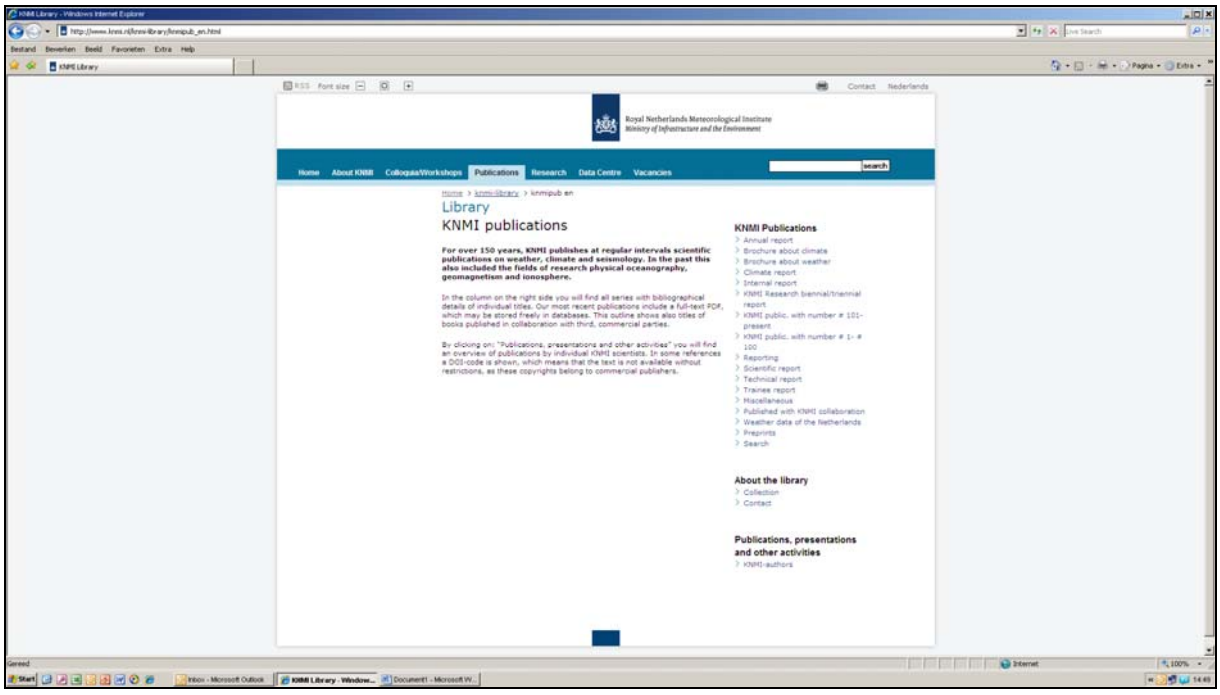

The most recent reports are available as a PDF on this site.